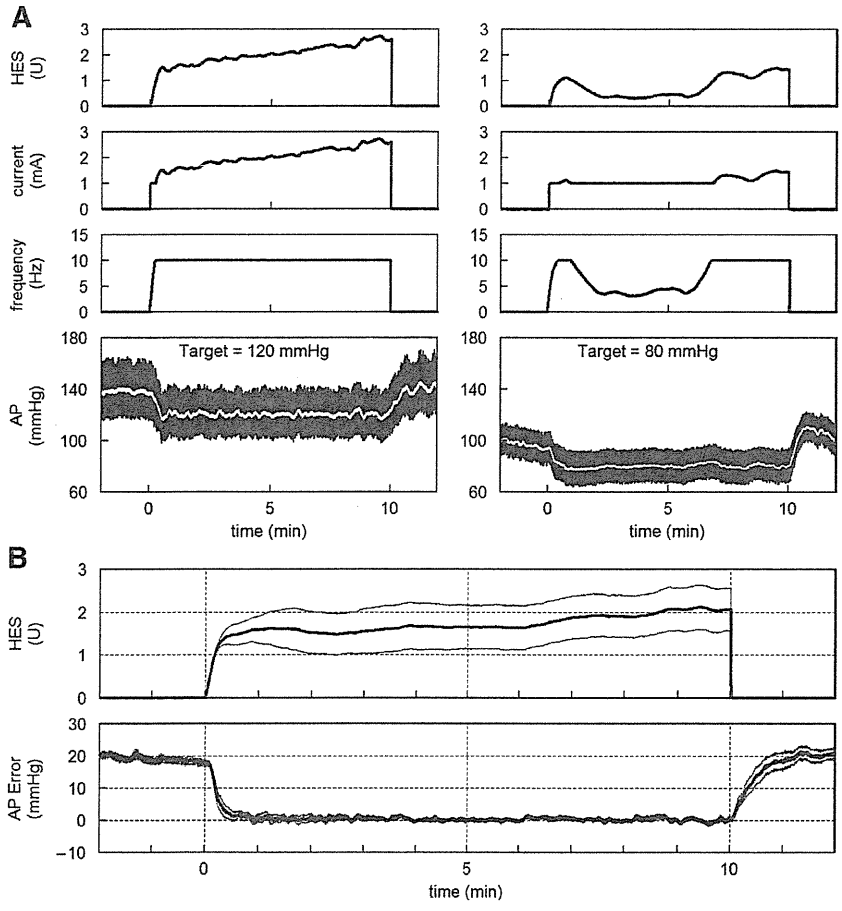

Figure 5. (**A**) Results of 10-min feedback control of arterial pressure (AP) by hind-limb electrical stimulation (HES) obtained from 2 cats. In each cat, the target AP was set at 20 mmHg below the baseline AP value. The current and frequency of HES were automatically adjusted to keep the AP at the target level. (**B**) HES command and the error signal between the target AP and measured AP averaged from 8 cats. The thick and thin lines indicate mean ± SE values, respectively.

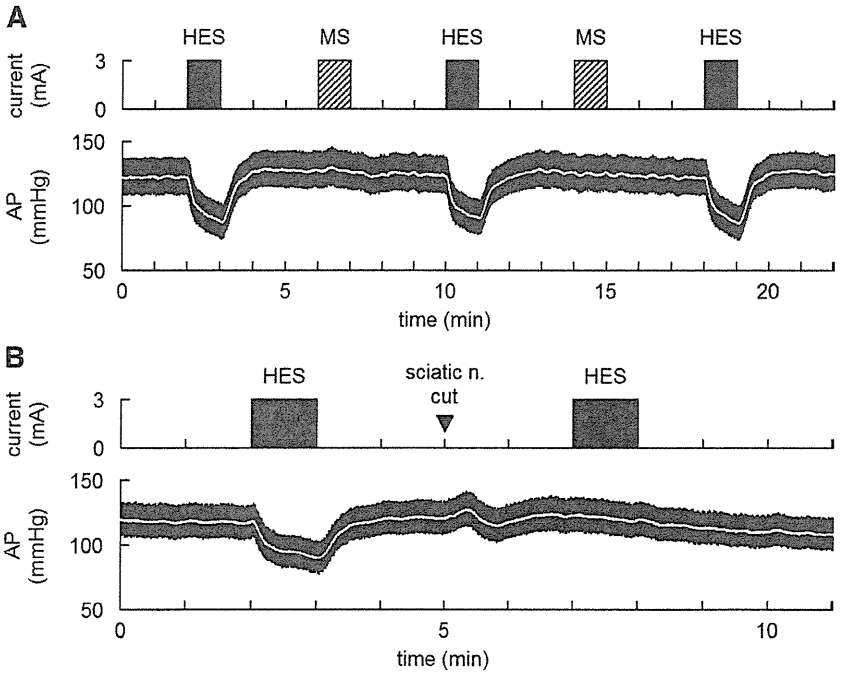

Figure 6. (**A**) Effects of electrical stimulation of the triceps surae muscle (MS) in comparison to hind-limb electrical stimulation (HES). Although muscle twitching was observed, there was no change in arterial pressure (AP) during MS. (**B**) Effects of sectioning the ipsilateral sciatic nerve on the HES-induced changes in AP. After the severance of the ipsilateral sciatic nerve, HES no longer produced significant hypotension.

from 1 to 7 min of the 10-min regulation. In this time period, the HES command altered the stimulus frequency rather than the stimulus current.

Mean and mean ± SE values of the HES command averaged from 8 animals are shown in the top panel of **Figure 5B**. There was a large variance in the HES command among the animals, suggesting inter-individual differences in the responsiveness to HES. The target AP was 102.5±5.6 mmHg across the animals. The error signal between the target AP and measured AP disappeared in less than 1 min (**Figure 5B**,

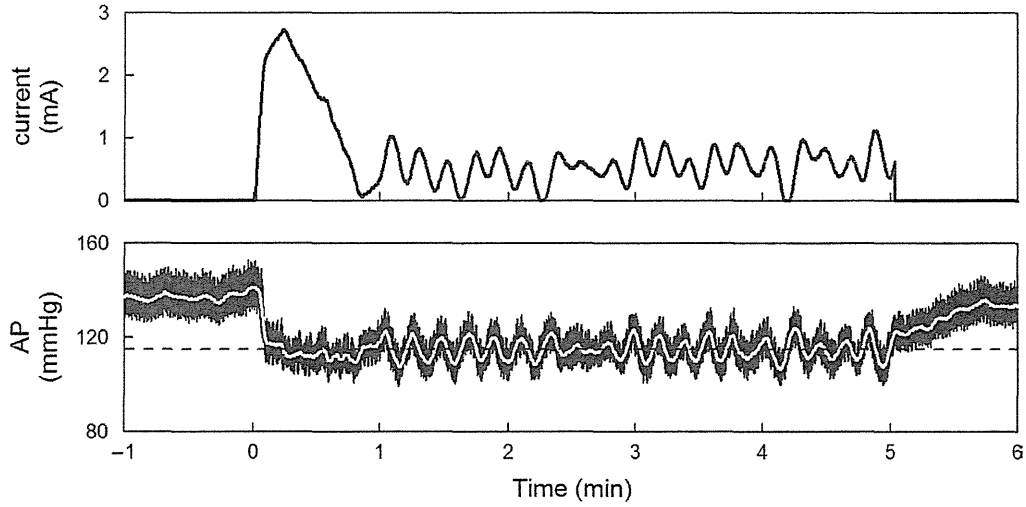

Figure 7. Typical recordings showing failure of controlling the intensity of the hind-limb electrical stimulation during the course of controller development. In this experimental run, only the stimulus current was controlled with a fixed stimulus frequency at 10 Hz. The controller showed on–off type controller behavior once the arterial pressure (AP) approached the target level. The horizontal dashed line indicates the target AP level.

Bottom). The time required for the AP response to reach 90% of the target AP decrease was 38±10 s. Thereafter, the error remained very small until the end of the 10-min regulation. The standard deviation of the steady-state error was 1.3±0.1 mmHg. After the end of the feedback regulation, the error signal gradually returned to approximately 20 mmHg.

Figure 6 represents typical results of the supplemental protocols. Electrical stimulation of the triceps surae muscle (denoted as "MS") did not change AP significantly in spite of visible twitching of the stimulated muscle, suggesting that the depressor response to HES was not the outcome of the direct muscle stimulation (**Figure 6A**). Sectioning the ipsilateral sciatic nerve abolished the depressor effect of HES, suggesting that somatic afferent signals were delivered through the sciatic nerve to the central nervous system during HES (**Figure 6B**).

Discussion

We identified the dynamic input–output relationship between HES and the AP response. By using the model transfer function from HES to AP, we were able to develop a servo-controller that automatically adjusted the HES command to reduce AP at a prescribed target level.

Development of the Feedback Controller

The stimulus current-AP response relationship showed a monotonous decreasing slope (**Figure 2C**). Because the effect of the pulse width was statistically insignificant, we chose the stimulus current as a primary control variable. The problem with using the stimulus current for the control variable was that a certain threshold current existed between 0 and 1 mA where the AP response to HES became discontinuous. If the stimulus current happened to be feedback controlled near the threshold current, AP showed significant oscillation around the target level (**Figure 7**, see Appendix B for details). To avoid such a problem related to the threshold current, we set the minimum current to 1 mA (above the threshold current) and used the stimulus frequency as a secondary control variable (**Figure 4B**).

The stimulus frequency-AP response relationship revealed a valley-shaped curve with the nadir of approximately 10 Hz (**Figure 2D**). The result is similar to that obtained by stimulating hamstring muscle afferent nerves.[26] From the viewpoint of controller design, the valley-shaped input–output relationship is troublesome because the proportional-integral controller only assumes a monotonous input–output relationship.[23] To avoid the problem of the valley-shaped input–output relationship, we limited the stimulus frequency to the range from 0 to 10 Hz (**Figure 4B, Right**). A similar strategy of selecting the monotonous input–output portion was used in a previous study.[12]

We quantified the dynamic AP response to HES using a transfer function analysis (**Figure 3B**), and modeled it by a second-order low-pass filter with a pure dead time (**Figure 3C**). Once the transfer function is modeled, we could construct a numerical simulator for the feedback controller design (**Figure 4A**). Because the optimization of control parameters usually requires a number of trials, even if the initial values are selected via classical methods such as the Ziegler–Nichols' method,[23] it is impractical to determine optimal parameter values without using the simulator. The simulation results indicated that the integral gain value of 0.005 would provide rapid and stable AP regulation (**Figure 4C**). Because the controller was designed via intensive simulations, AP was actually controlled at the target level with a small variance (**Figure 5B, Bottom**). Note that the current and frequency of HES were automatically adjusted and individualized via the feedback mechanism (**Figure 5A**).

Bionic Strategies Using Neural Interfaces

A framework of treating cardiovascular diseases using neural interfaces is intriguing because the autonomic nervous system exerts powerful influences on the circulatory system. In previous studies, we identified the dynamic characteristics of the arterial baroreflex system and used them to design an artificial vasomotor center. The artificial vasomotor center was able to control AP by stimulating the celiac ganglia in anesthetized rats[10,11] or the spinal cord in anesthetized cats.[12] The strength and rapidity of the neural effect on the cardiovascular system compared with that of the

humoral effect[27,28] make the neural interventions desirable for the rapid and stable restoration of AP against acute disturbances such as those induced by postural changes. Gotoh et al demonstrated that a direct neural interface to the rostral ventrolateral medulla also enabled rapid and stable restoration of AP during nitroprusside-induced hypotension in conscious rats?[29] The bionic system to control AP has also been applied in human subjects![13]

Although the aforementioned bionic systems aimed to maintain AP against acute hypotension by increasing sympathetic nerve activity,[10–13,29] sympathoinhibition might also be required for the treatment of cardiovascular diseases accompanying sympathetic overactivity. Baroreceptor activation is one of the potential sympathoinhibitory neural modulation?[8,9] In the present study we only demonstrated a framework of short-term AP control by HES. With a development of proper implanting electrodes, however, we might be able to control AP chronically using HES. Although carotid sinus baroreceptor stimulation has a potential to treat drug-resistant hypertension,[9] it could activate peripheral chemoreflex by stimulating carotid bodies. HES might circumvent such unintentional chemoreflex activation. Another clinical implication will be the treatment of chronic heart failure. Although the vagal effect of HES was not evaluated in the present study, acupuncture stimulation might facilitate cardiac vagal activity?[30] Because chronic intermittent vagal nerve stimulation increased the survival of chronic heart failure rats,[7] chronic intermittent HES might be used as an alternative method of direct vagal nerve stimulation for the treatment of chronic heart failure.

Study Limitations

First, we did not identify the mechanism of HES. Because sectioning of the ipsilateral sciatic nerve abolished the AP response to HES (**Figure 6B**), somatic afferent is involved in the effect of HES. In a series of studies, Chao et al and Li et al demonstrated that electroacupuncture activated group III and IV fibers in the median nerves and inhibited sympathetic outflow via activation of μ- and δ-opioid receptors in the rostral ventrolateral medulla?[31,32] Whether a similar mechanism underlies in the rapid-onset and short-lasting effect of HES awaits further studies.

Second, we used pentobarbital anesthesia. Although peripheral neurotransmissions of norepinephrine and acetylcholine can be assessed under the same anesthesia,[28,33] because pentobarbital can suppress many neurotransmitters in the central nervous system,[34] anesthesia might compromise the HES effect. Further studies are required to establish the utility of HES in awake conditions.

Third, we set the proportional gain of the controller at zero to avoid pulsatile changes in the HES command. However, other approaches such as that using a low-passed signal of measured AP as a controlled variable might also be effective to avoid the pulsatile variation in the HES command.

Finally, a development of implanting electrodes is the prerequisite for chronic use of HES. Intramuscular electrodes used in functional electrical stimulation might be used for HES but further refinements are clearly needed regarding the positioning of electrodes including the depth of implantation?[35,36]

In conclusion, we identified the dynamic characteristics of the AP response to acupuncture-like HES and demonstrated that a servo-controlled HES system was able to reduce AP at a prescribed target level. Although further studies are required to identify the mechanism of HES to reduce AP, acupuncture-like HES would be an additional modality to exert a quantitative depressor effect on the cardiovascular system.

Acknowledgments

This study was supported by the following Grants: "Health and Labour Sciences Research Grant for Research on Advanced Medical Technology", "Health and Labour Sciences Research Grant for Research on Medical Devices for Analyzing, Supporting and Substituting the Function of Human Body", "Health and Labour Sciences Research Grant (H18-Iryo-Ippan-023) (H18-Nano-Ippan-003) (H19-Nano-Ippan-009)", from the Ministry of Health, Labour and Welfare of Japan, and the "Industrial Technology Research Grant Program" from New Energy and Industrial Technology Development Organization of Japan.

References

1. Bilgutay AM, Bilgutay IM, Merkel FK, Lillehei CW. Vagal tuning: A new concept in the treatment of supraventricular arrhythmias, angina pectoris, and heart failure. *J Thorac Cardiovasc Surg* 1968; **56:** 71–82.
2. Braunwald E, Epstein SE, Glick G, Wechsler AS, Braunwald NS. Relief of angina pectoris by electrical stimulation of the carotid-sinus nerves. *N Engl J Med* 1967; **277:** 1278–1283.
3. Schwartz SI, Griffith LS, Neistadt A, Hagfors N. Chronic carotid sinus nerve stimulation in the treatment of essential hypertension. *Am J Surg* 1967; **114:** 5–15.
4. Vanoli E, De Ferrari GM, Stramba-Badiale M, Hull SS Jr, Foreman RD, Schwartz PJ. Vagal stimulation and prevention of sudden death in conscious dogs with a healed myocardial infarction. *Circ Res* 1991; **68:** 1471–1481.
5. Yang JL, Chen GY, Kuo CD. Comparison of effect of 5 recumbent positions on autonomic nervous modulation in patients with coronary artery disease. *Circ J* 2008; **72:** 902–908.
6. Baba R, Koketsu M, Nagashima M, Inasaka H, Yoshinaga M, Yokota M. Adolescent obesity adversely affects blood pressure and resting heart rate. *Circ J* 2007; **71:** 722–726.
7. Li M, Zheng C, Sato T, Kawada T, Sugimachi M, Sunagawa K. Vagal nerve stimulation markedly improves long-term survival after chronic heart failure in rats. *Circulation* 2004; **109:** 120–124.
8. Zucker IH, Hackley JF, Cornish KG, Hiser BA, Anderson NR, Kieval R, et al. Chronic baroreceptor activation enhances survival in dogs with pacing-induced heart failure. *Hypertension* 2007; **50:** 904–910.
9. Mohaupt MG, Schmidli J, Luft FC. Management of uncontrollable hypertension with a carotid sinus stimulation device. *Hypertension* 2007; **50:** 825–828.
10. Sato T, Kawada T, Shishido T, Sugimachi M, Alexander J Jr, Sunagawa K. Novel therapeutic strategy against central baroreflex failure: A bionic baroreflex system. *Circulation* 1999; **100:** 299–304.
11. Sato T, Kawada T, Sugimachi M, Sunagawa K. Bionic technology revitalizes native baroreflex function in rats with baroreflex failure. *Circulation* 2002; **106:** 730–734.
12. Yanagiya Y, Sato T, Kawada T, Inagaki M, Tatewaki T, Zheng C, et al. Bionic epidural stimulation restores arterial pressure regulation during orthostasis. *J Appl Physiol* 2004; **97:** 984–990.
13. Yamasaki F, Ushida T, Yokoyama T, Ando M, Yamashita K, Sato T. Artificial baroreflex: Clinical application of a bionic baroreflex system. *Circulation* 2006; **113:** 634–639.
14. Li P, Pitsillides KF, Rendig SV, Pan HL, Longhurst JC. Reversal of reflex-induced myocardial ischemia by median nerve stimulation: A feline model of electroacupuncture. *Circulation* 1998; **97:** 1186–1194.
15. Longhurst JC. Electroacupuncture treatment of arrhythmias in myocardial ischemia. *Am J Physiol Heart Circ Physiol* 2007; **292:** H2032–H2034.
16. Lujan HL, Kramer VJ, DiCarlo SE. Electroacupuncture decreases the susceptibility to ventricular tachycardia in conscious rats by reducing cardiac metabolic demand. *Am J Physiol Heart Circ Physiol* 2007; **292:** H2550–H2555.
17. Ohsawa H, Okada K, Nishijo K, Sato Y. Neural mechanism of depressor responses of arterial pressure elicited by acupuncture-like stimulation to a hindlimb in anesthetized rats. *J Auton Nerv Syst* 1995; **51:** 27–35.
18. Uchida S, Shimura M, Ohsawa H, Suzuki A. Neural mechanism of bradycardiac responses elicited by acupuncture-like stimulation to a hind limb in anesthetized rats. *J Physiol Sci* 2007; **57:** 377–382.
19. Michikami D, Kamiya A, Kawada T, Inagaki M, Shishido T, Yamamoto K, et al. Short-term electroacupuncture at Zusanli resets the arterial baroreflex neural arc toward lower sympathetic nerve

activity. *Am J Physiol Heart Circ Physiol* 2006; **291:** H318–H326.
20. Yamamoto H, Kawada T, Kamiya A, Kita T, Sugimachi M. Electroacupuncture changes the relationship between cardiac and renal sympathetic nerve activities in anesthetized cats. *Auton Neurosci: Basic and Clinical* 2008; **144:** 43–49.
21. Marmarelis PZ, Marmarelis VZ. Analysis of Physiological Systems. The white noise method in system identification. New York: Plenum; 1978.
22. Snedecor GW, Cochran WG. Statistical Methods, 8th ed. Ames, Iowa: University Press; 1989.
23. Åström K, Hägglund T. PID Controllers: Theory, Design, and Tuning, 2nd ed. City of Publication: Instrument Society of America; 1995.
24. Kawada T, Sunagawa G, Takaki H, Shishido T, Miyano H, Miyashita H, et al. Development of a servo-controller of heart rate using a treadmill. *Jpn Circ J* 1999; **63:** 945–950.
25. Kawada T, Ikeda Y, Takaki H, Sugimachi M, Kawaguchi O, Shishido T, et al. Development of a servo-controller of heart rate using a cycle ergometer. *Heart Vessels* 1999; **14:** 177–184.
26. Johansson B. Circulatory responses to stimulation of somatic afferents with special reference to depressor effects from muscle nerves. *Acta Physiol Scand* 1962; **Suppl 198:** 1–91.
27. Kawada T, Miyamoto T, Miyoshi Y, Yamaguchi S, Tanabe Y, Kamiya A, et al. Sympathetic neural regulation of heart rate is robust against high plasma catecholamines. *J Physiol Sci* 2006; **56:** 235–245.
28. Kawada T, Yamazaki T, Akiyama T, Shishido T, Miyano H, Sato T, et al. Interstitial norepinephrine level by cardiac microdialysis correlates with ventricular contractility. *Am J Physiol Heart Circ Physiol* 1997; **273:** H1107–H1112.
29. Gotoh TM, Tanaka K, Morita H. Controlling arterial blood pressure using a computer-brain interface. *Neuroreport* 2005; **16:** 343–347.
30. Nishijo K, Mori H, Yosikawa K, Yazawa K. Decreased heart rate by acupuncture stimulation in humans via facilitation of cardiac vagal activity and suppression of cardiac sympathetic nerve. *Neurosci Lett* 1997; **227:** 165–168.
31. Chao DM, Shen LL, Tjen-A-Looi S, Pitsillides KF, Li P, Longhurst JC. Naloxone reverses inhibitory effect of electroacupuncture on sympathetic cardiovascular reflex responses. *Am J Physiol Heart Circ Physiol* 1999; **276:** H2127–H2134.
32. Li P, Tjen-A-Looi SC, Longhurst JC. Rostral ventrolateral medullary opioid receptor subtypes in the inhibitory effect of electroacupuncture on reflex autonomic response in cats. *Auton Neurosci: Basic and Clinical* 2001; **89:** 38–47.
33. Kawada T, Yamazaki T, Akiyama T, Li M, Ariumi H, Mori H, et al. Vagal stimulation suppresses ischemia-induced myocardial interstitial norepinephrine release. *Life Sci* 2006; **78:** 882–887.
34. Adachi YU, Yamada S, Satomoto M, Watanabe K, Higuchi H, Kazama T. et al. Pentobarbital inhibits L-DOPA-induced dopamine increases in the rat striatum: An in vivo microdialysis study. *Brain Res Bull* 2006; **69:** 593–596.
35. Guevremont L, Norton JA, Mushahwar VK. Physiologically based controller for generating overground locomotion using functional electrical stimulation. *J Neurophysiol* 2007; **97:** 2499–2510.
36. Hardin E, Kobetic R, Murray L, Corado-Ahmed M, Pinault G, Sakai J, et al. Walking after incomplete spinal cord injury using an implanted FES system: A case report. *J Rehabil Res Dev* 2007; **44:** 333–346.

Appendix A

Framework of the Feedback Controller

Figure 4A is a simplified block diagram of the feedback controller system used in the present study. The controller was based on a proportional-integral controller[23–25] $G(f)$ represents the transfer function of the controller.

$$G(f)=-K_P+\frac{-K_I}{2\pi fj} \quad \text{(A1)}$$

where K_P and K_I denote proportional and integral gains, respectively. j represents the imaginary unit. Negative signs for the proportional and integral gains compensate for the negative input–output relationship between HES and the AP response. $H(f)$ represents a model transfer function from HES to AP determined from Protocol 3. The measured AP can be expressed as:

$$AP_{Measured}(f)=H(f)HES(f)+AP_{Noise}(f) \quad \text{(A2)}$$

where $AP_{Noise}(f)$ is the AP fluctuation such as that associated with changes in animal conditions. The controller compares the measured AP with the target AP, and adjusts the HES command to minimize the difference between them according to the following equation:

$$HES(f)=G(f)[AP_{Target}(f)-AP_{Measured}(f)] \quad \text{(A3)}$$

By eliminating $HES(f)$ from the equations A2 and A3, the overall controller characteristics are described as:

$$AP_{Measured}(f)=\frac{G(f)H(f)}{1+G(f)H(f)}AP_{Target}(f)+\frac{1}{1+G(f)H(f)}AP_{Noise}(f) \quad \text{(A4)}$$

The equation A4 indicates that if $G(f)$ is properly selected so that $G(f)\,H(f)$ becomes by far greater than unity, the measured AP approaches the target AP whereas the noise term is significantly attenuated over the frequency range of interest.

Appendix B

Problem with the Threshold Current

We tried to adjust the intensity of HES by the stimulus current alone. When the stimulus current happened to be feedback controlled near a threshold current, however, the controller showed an on–off type controller behavior around the target AP level, as shown in **Figure 7**. At time zero, the controller was activated. The stimulus current increased to approximately 2.7 mA in the beginning and then decreased to a value below 1 mA, accompanying the AP reduction around a target level (a horizontal dashed line). However, the stimulus current and AP did not stabilize. Because the AP response was discontinuous at the threshold current (ie, the depressor effect of HES was abruptly turned on and off), the controller could not adjust the stimulus current in a continuous manner. To avoid this kind of on–off type controller behavior, we introduced the stimulus frequency as the secondary control variable (**Figure 4B**).

J Physiol Sci (2009) 59:447–455
DOI 10.1007/s12576-009-0055-5

ORIGINAL PAPER

High levels of circulating angiotensin II shift the open-loop baroreflex control of splanchnic sympathetic nerve activity, heart rate and arterial pressure in anesthetized rats

Toru Kawada · Atsunori Kamiya · Meihua Li · Shuji Shimizu · Kazunori Uemura · Hiromi Yamamoto · Masaru Sugimachi

Received: 21 May 2009 / Accepted: 19 July 2009 / Published online: 18 August 2009

Abstract Although an acute arterial pressure (AP) elevation induced by intravenous angiotensin II (ANG II) does not inhibit sympathetic nerve activity (SNA) compared to an equivalent AP elevation induced by phenylephrine, there are conflicting reports as to how circulating ANG II affects the baroreflex control of SNA. Because most studies have estimated the baroreflex function under closed-loop conditions, differences in the rate of input pressure change and the magnitude of pulsatility may have biased the estimation results. We examined the effects of intravenous ANG II (10 μg kg^{-1} h^{-1}) on the open-loop system characteristics of the carotid sinus baroreflex in anesthetized and vagotomized rats. Carotid sinus pressure (CSP) was raised from 60 to 180 mmHg in increments of 20 mmHg every minute, and steady-state responses in systemic AP, splanchnic SNA and heart rate (HR) were analyzed using a four-parameter logistic function. ANG II significantly increased the minimum values of AP (67.6 ± 4.6 vs. 101.4 ± 10.9 mmHg, $P < 0.01$), SNA (33.3 ± 5.4 vs. 56.5 ± 11.5%, $P < 0.05$) and HR (391.1 ± 13.7 vs. 417.4 ± 11.5 beats/min, $P < 0.01$). ANG II, however, did not attenuate the response range for AP (56.2 ± 7.2 vs. 49.7 ± 6.2 mmHg), SNA (69.6 ± 5.7 vs. 78.9 ± 9.1%) or HR (41.7 ± 5.1 vs. 51.2 ± 3.8 beats/min). The maximum gain was not affected for AP (1.57 ± 0.28 vs. 1.20 ± 0.25), SNA (1.94 ± 0.34 vs. 2.04 ± 0.42%/mmHg) or HR (1.11 ± 0.12 vs. 1.28 ± 0.19 beats min^{-1} $mmHg^{-1}$). It is concluded that high levels of circulating ANG II did not attenuate the response range of open-loop carotid sinus baroreflex control for AP, SNA or HR in anesthetized and vagotomized rats.

Keywords Systems analysis · Open-loop gain · Equilibrium diagram · Carotid sinus baroreflex · Rats

T. Kawada (✉) · A. Kamiya · M. Li · S. Shimizu · K. Uemura · M. Sugimachi
Department of Cardiovascular Dynamics, Advanced Medical Engineering Center, National Cardiovascular Center Research Institute, 5-7-1 Fujishirodai, Suita, Osaka 565-8565, Japan
e-mail: torukawa@res.ncvc.go.jp

M. Li · S. Shimizu
Japan Association for the Advancement of Medical Equipment, Tokyo 113-0033, Japan

H. Yamamoto
Division of Cardiology, Department of Internal Medicine, Kinki University School of Medicine, Osaka 589-8511, Japan

Introduction

The arterial baroreflex is an important negative feedback system that stabilizes systemic arterial pressure (AP) during daily activities. The sympathetic arterial baroreflex can be divided into the neural and peripheral arc subsystems [1]. The neural arc characterizes the input–output relation between the baroreceptor pressure input and efferent sympathetic nerve activity (SNA), whereas the peripheral arc defines the input–output relation between SNA and AP. These subsystems operate as a controller and a plant, respectively, in the negative feedback loop. Although the input signal to the neural arc is primarily the absolute input pressure level, the rate of input pressure change [1–3] and the magnitude of pulsatility [4–7] are also important input signals that critically affect the baroreflex function. Many investigators employ pharmacologic interventions, such as intravenous phenylephrine and nitroprusside administration, to estimate baroreflex function under closed-loop conditions. The rate of input pressure change and the

magnitude of pulsatility, however, may vary within and between studies, which could bias the estimation results. In addition, experiments performed under baroreflex closed-loop conditions do not usually permit an evaluation of the baroreflex control of AP, because measured AP cannot be separated into signals for the input pressure and output pressure. An open-loop experiment with isolated baroreceptor regions is therefore required to evaluate the baroreflex function precisely.

Angiotensin II (ANG II) can affect the arterial baroreflex by centrally increasing sympathetic outflow, stimulating sympathetic ganglia and the adrenal medulla, and facilitating neurotransmission at sympathetic nerve endings [8]. Although an acute AP elevation induced by intravenous ANG II does not inhibit SNA compared to an equivalent AP elevation induced by phenylephrine, how circulating ANG II affects the baroreflex control of SNA varies among reports, i.e., intravenous ANG has been shown to attenuate [9, 10] or not attenuate [11, 12] the baroreflex control of SNA. Because it is related to the pathologic sympathoexcitation observed in such cardiovascular diseases as chronic heart failure [13], analyzing the effects of circulating ANG II on the baroreflex open-loop system characteristics will deepen our understanding of the pathologic roles of ANG II. In the present study, we examined the effects of intravenous ANG II (10 $\mu g\ kg^{-1}\ h^{-1}$ or 167 $ng\ kg^{-1}\ min^{-1}$) on the open-loop system characteristics of the baroreflex neural and peripheral arcs in anesthetized rats. We hypothesized that ANG II would increase the minimum SNA and attenuate the range of SNA response because the maximum SNA may be saturated. Contrary to our hypothesis, ANG II increased both the minimum and maximum SNA, preserving the range of SNA response controlled by the arterial baroreflex.

Materials and methods

Animals were cared for in strict accordance with the guiding principles for the care and use of animals in the field of physiological sciences, which has been approved by the Physiological Society of Japan. All experimental protocols were reviewed and approved by the Animal Subjects Committee at the National Cardiovascular Center.

Baroreflex open-loop experiment

Male Sprague–Dawley rats ($n = 8$, 482 ± 14 g body weight, mean $\pm$ SE) were anesthetized with an intraperitoneal injection (2 ml/kg) of a mixture of urethane (250 mg/ml) and α-chloralose (40 mg/ml), and mechanically ventilated with oxygen-enriched room air. A venous catheter was inserted into the right femoral vein, and a tenfold dilution of the anesthetic mixture was administered ($2\ ml\ kg^{-1}\ h^{-1}$) to maintain an appropriate level of anesthesia. An arterial catheter was inserted into the right femoral artery to measure AP. A cardiotachometer was used to measure heart rate (HR). Another venous catheter was inserted into the left femoral vein to administer Ringer's solution with or without ANG II.

We exposed a postganglionic branch of the splanchnic nerve through a left flank incision and attached a pair of stainless steel wire electrodes (Bioflex wire AS633, Cooner Wire, CA) to record SNA. The nerve and electrodes were covered with silicone glue (Kwik-Sil, World Precision Instruments, Sarasota, FL) for insulation and fixation. To quantify the nerve activity, the preamplified nerve signal was band-pass filtered at 150–1,000 Hz, and then full-wave rectified and low-pass filtered with a cutoff frequency of 30 Hz. Pancuronium bromide ($0.4\ mg\ kg^{-1}\ h^{-1}$) was administered to prevent muscular activity from contaminating the SNA recording. At the end of the experiment, we confirmed the disappearance of SNA after an intravenous bolus injection of hexamethonium bromide (60 mg/kg) and recorded the noise level.

The vagal and aortic depressor nerves were sectioned at the neck to avoid reflexes from the cardiopulmonary region and aortic arch. The bilateral carotid sinuses were isolated from the systemic circulation according to previously reported procedures [14, 15]. Briefly, a fine needle with a 7-0 polypropylene suture (PROLENE, Ethicon, GA, USA) was passed through the tissue between the external and internal carotid arteries, and the external carotid artery was ligated close to the carotid bifurcation. The internal carotid artery was embolized using two or three bearing balls (0.8 mm in diameter, Tsubaki Nakashima, Nara, Japan), which were injected from the common carotid artery. The isolated carotid sinuses were filled with warmed Ringer's solution through catheters inserted via the common carotid arteries. Carotid sinus pressure (CSP) was controlled using a servo-controlled piston pump. Heparin sodium (100 U/kg) was given intravenously to prevent blood coagulation. Body temperature was maintained at approximately 38°C with a heating pad.

Protocols

Sympathetic nerve activity and AP responses to CSP perturbations were monitored for at least 30 min after the surgical preparation was completed. If these responses became smaller within this period, the animal was discarded from the study. Possible causes for deteriorations in the responses include surgical damage to the carotid sinus nerves and brain ischemia due to bilateral carotid occlusion.

The CSP was decreased to 60 mmHg for 4–6 min, and then increased every minute from 60 to 180 mmHg using 20-mmHg increments. At least four step cycles were performed under control conditions while Ringer's solution was continuously administered (6 ml kg^{-1} h^{-1}). After recording the control data, the intravenous Ringer's solution was replaced with that containing ANG II (167 ng kg^{-1} min^{-1}). The dose of ANG II was chosen to induce a significant pressor effect based on previous studies [16, 17]. At least three step cycles were performed during ANG II administration.

Data analysis

Data were sampled at 200 Hz using a 16-bit analog-to-digital converter and stored on the hard disk of a dedicated laboratory computer system. To quantify the open-loop static characteristics of the carotid sinus baroreflex, mean values of SNA, AP and HR were calculated during the last 10 s at each CSP level. The effects of ANG II were assessed during the third step cycle after ANG II administration began, at which point the hemodynamic responses to ANG II appeared to reach steady state. Comparisons were made against two control step cycles (control 1 and control 2, see Fig. 1). In each animal, the SNA noise level recorded after the administration of hexamethonium bromide was set to zero. The SNA values obtained at a CSP level of 60 mmHg during control 1 and control 2 were averaged and defined as 100%.

The open-loop characteristics of the AP, SNA and HR responses as functions of CSP were quantified by fitting a four-parameter logistic function to the obtained data as follows [18]:

$$y = \frac{P_1}{1 + \exp[P_2(\mathrm{CSP} - P_3)]} + P_4.$$

where y represents AP, SNA or HR; P_1 is the response range (the difference between the maximum and minimum values of y); P_2 is a slope coefficient; P_3 is the midpoint in CSP; P_4 is the minimum value of y. The maximum gain or maximum slope of the sigmoidal curve was obtained from $P_1P_2/4$.

The open-loop characteristics of the baroreflex peripheral arc (i.e., SNA–AP relation) were quantified using linear regression analysis as follows:

$$\mathrm{AP} = a \times \mathrm{SNA} + b.$$

where a and b represent the slope and intercept of the regression line, respectively.

Statistical analysis

All parameters were compared among control 1, control 2 and ANG II conditions using repeated-measures analysis of variance [19]. When there was a significant difference among the three conditions, all pairwise comparisons were performed using the Student-Neuman-Keuls test. Differences were considered significant at $P < 0.05$. All data are expressed as mean and SE values.

Results

Typical experimental recordings are shown in Fig. 1. The stepwise input from 60 to 180 mmHg was imposed repeatedly on CSP. An increase in CSP decreased SNA. m-SNA represents the 5-s moving-average signal of the percentage of SNA. AP and HR were also decreased in response to increases in CSP. After ANG II administration was initiated, the levels of SNA, AP and HR all increased compared to the levels before ANG II administration. The responses in SNA, AP and HR to the CSP input appeared to be preserved. Data obtained from the three boxes with dashed lines (control 1, control 2 and ANG II) were used for the statistical analysis.

The open-loop characteristics of the total baroreflex revealed sigmoidal nonlinearity (Fig. 2a). No significant differences were observed between the two control conditions. ANG II significantly increased the minimum AP without affecting the response range, slope coefficient or midpoint in CSP (Table 1). The maximum gain of the total baroreflex was unchanged. The open-loop characteristics of the baroreflex control of HR also approximated sigmoidal nonlinearity (Fig. 2b), and no significant differences were observed between the two control conditions. ANG II significantly increased the minimum HR without affecting the response range, slope coefficient or midpoint in CSP (Table 1). The maximum slope of the baroreflex control of HR was unchanged.

The total baroreflex was decomposed into the neural and peripheral arc subsystems. The open-loop characteristics of the baroreflex neural arc revealed sigmoidal nonlinearity (Fig. 3a). There were no significant differences between the two control conditions. ANG II significantly increased the minimum SNA (Table 1). Although the midpoint in CSP was lower in ANG II than in control 1, the difference was not significant when compared with control 2. ANG II did not affect the response range, slope coefficient or the maximum slope of the baroreflex control of SNA. The open-loop characteristics of the baroreflex peripheral arc approximated a straight line (Fig. 3b). There were no significant differences between the two control conditions. ANG II significantly increased the intercept of the regression line (Table 1). AP at 100% SNA did not change significantly, suggesting that the slope of the regression line could be shallower under the ANG II condition. The slope of the

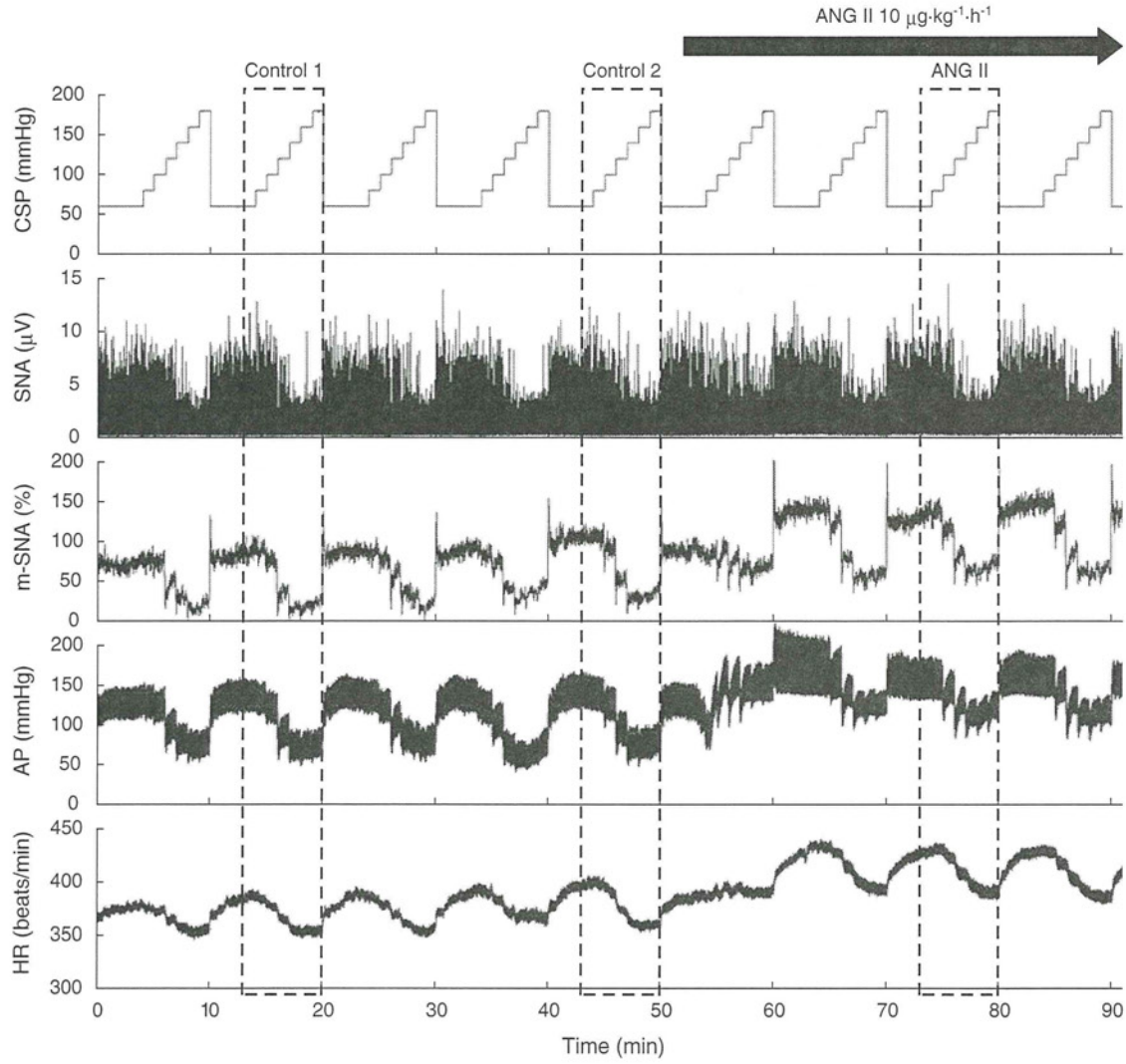

Fig. 1 Typical recordings of carotid sinus pressure (*CSP*), splanchnic sympathetic nerve activity (*SNA*), the 5-s moving-average signal of the percentage of SNA (*m-SNA*), systemic arterial pressure (*AP*) and heart rate (*HR*). CSP was changed stepwise from 60 to 180 mmHg in 20-mmHg increments every minute. Angiotensin II (ANG II) was administered intravenously while the CSP perturbation was continued. ANG II significantly increased SNA, AP and HR. Reflex responses in SNA, AP and HR were not attenuated in the presence of ANG II. *Dashed boxes* indicate the step cycles used for the statistical analysis

regression line, however, was not statistically different among the three conditions.

An equilibrium diagram or a balance diagram was obtained by drawing the neural and peripheral arcs using SNA as the common abscissa and CSP or AP as an ordinate [20–22]. Figure 4 illustrates the equilibrium diagrams under the control 2 (dashed line) and ANG II (solid line) conditions, which were drawn based on the mean parameter values from the logistic function and regression line. Open and filled circles represent the closed-loop operating points under the control 2 and ANG II conditions, respectively. Although AP at the closed-loop operating point was significantly increased by the intravenous ANG II, SNA at the closed-loop operating point was unchanged (Table 1). If ANG II affected the peripheral arc alone, the closed-operating point may have been located at the point depicted by the open triangle. If ANG II affected the neural arc alone, the closed-loop operating point may have been located at the point depicted by the filled triangle.

Discussion

Effects of ANG II on open-loop baroreflex control of SNA

Intravenous ANG II at 167 ng kg^{-1} min^{-1} shifted the open-loop baroreflex control of splanchnic SNA toward higher SNA values without attenuating the size of the response range (Fig. 3a; Table 1). The maximum slope was

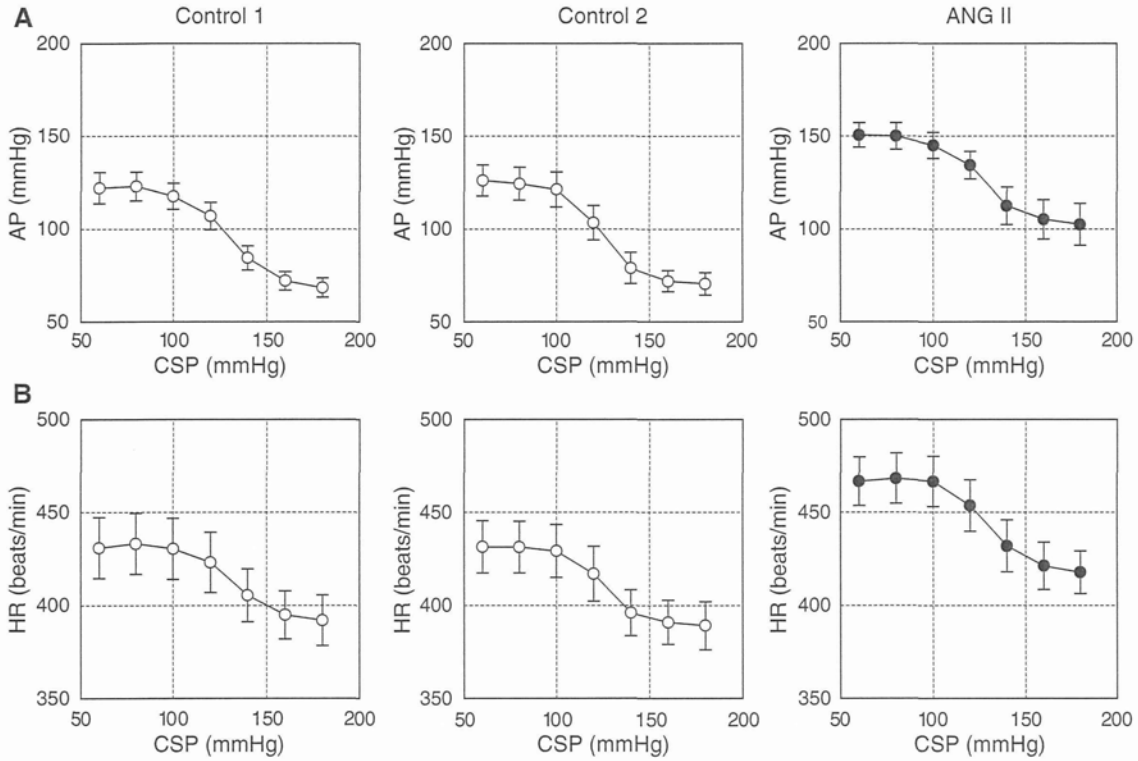

Fig. 2 **a** Averaged input–output relation of the total baroreflex. AP decreased in response to an increase in the CSP. ANG II increased AP, while the range of the AP response was preserved. **b** Averaged input–output relation of the arterial baroreflex control of HR. HR decreased in response to an increase in the CSP. ANG II increased the HR, while the range of the HR response was preserved

unaltered, which agreed with a previous study from our laboratory in which intravenous ANG II at 100 ng kg^{-1} min^{-1} did not change the dynamic gain of the neural arc in anesthetized rabbits [23]. In contrast, Sanderford and Bishop demonstrated that ANG II at 10 or 20 ng kg^{-1} min^{-1} significantly reduced the maximum renal SNA and attenuated the range of baroreflex control of renal SNA in conscious rabbits [9, 24]. On the other hand, Tan et al. [12] demonstrated that intravenous ANG II at 400 ng kg^{-1} min^{-1} did not increase the levels of renal SNA in anesthetized rats. The regional differences in SNA may partly explain the conflicting results, because Fukiyama [25] noted that ANG II infusion (3.5–9.5 ng kg^{-1} min^{-1}) through the vertebral artery resulted in an increase in splanchnic SNA, a transient increase followed by a decrease in renal SNA, and no change in cardiac SNA in anesthetized dogs.

Activation of the renin–angiotensin system contributes to the pathologic sympathoexcitation observed in such cardiovascular diseases as chronic heart failure. In addition to the augmented cardiac sympathetic reflex, impairment of the arterial baroreflex is thought to contribute to sympathoexcitation [13]. The present results indicate that ANG II may increase SNA, but it does not attenuate baroreflex control of SNA such that the magnitude of the SNA response to the input pressure change is preserved (Fig. 3a). ANG II also did not attenuate the gain of the total baroreflex estimated by the magnitude of the AP response to the input pressure change (Fig. 2a). Therefore, the observed weakening of the baroreflex reported in patients with chronic heart failure may not be readily explainable by an acute effect of high circulating levels of ANG II.

Several studies have demonstrated that ANG II-induced hypertension does not decrease SNA via the arterial baroreflex compared to equivalent hypertension induced by phenylephrine [10, 12, 26]. Although those results seem to be consistent with the idea that ANG II blunts the arterial baroreflex, the experimental protocol is confusing, and the interpretation could be wrong as follows. The intersection between the neural and peripheral arcs in the baroreflex equilibrium diagram conforms to the closed-loop operating point [21, 27, 28]. In the present study, ANG II significantly increased AP without significant changes in SNA at the closed-loop operating point (Fig. 4, open vs. filled circles; Table 1). If we calculate the baroreflex control of SNA based on ANG II-induced hypertension, therefore, we would incorrectly conclude that the baroreflex does not control SNA. If we observe the SNA response to changes in

Table 1 Effects of intravenous angiotensin II (ANG II) on the parameters of logistic functions and regression lines of the open-loop baroreflex characteristics

	Control 1	Control 2	ANG II
Total baroreflex, CSP–AP relation			
P_1 (mmHg)	56.2 ± 7.2	56.3 ± 6.4	49.7 ± 6.2
P_2 ($mmHg^{-1}$)	0.116 ± 0.019	0.118 ± 0.015	0.094 ± 0.013
P_3 (mmHg)	129.2 ± 3.5	124.5 ± 2.8	125.7 ± 3.2
P_4 (mmHg)	67.6 ± 4.6	69.7 ± 5.8	101.4 ± 10.9**,††
Maximum gain	1.57 ± 0.28	1.58 ± 0.22	1.20 ± 0.25
Baroreflex control of HR, CSP–HR relation			
P_1(beats/min)	41.7 ± 5.1	43.9 ± 6.2	51.2 ± 3.8
P_2 ($mmHg^{-1}$)	0.123 ± 0.027	0.133 ± 0.018	0.099 ± 0.013
P_3 (mmHg)	131.8 ± 3.8	125.8 ± 3.6	129.1 ± 2.6
P_4 (beats/min)	391.1 ± 13.7	388.0 ± 12.6	417.4 ± 11.5**,††
Maximum slope (beats min^{-1} $mmHg^{-1}$)	1.11 ± 0.12	1.39 ± 0.23	1.28 ± 0.19
Neural arc, CSP–SNA relation			
P_1 (%)	69.6 ± 5.7	66.5 ± 7.4	78.9 ± 9.1
P_2 ($mmHg^{-1}$)	0.110 ± 0.016	0.124 ± 0.015	0.098 ± 0.011
P_3 (mmHg)	133.2 ± 3.8	127.3 ± 3.1	126.0 ± 3.4*
P_4 (%)	33.3 ± 5.4	35.0 ± 6.4	56.5 ± 11.5*,†
Maximum slope (%/mmHg)	1.94 ± 0.34	2.02 ± 0.33	2.04 ± 0.42
Peripheral arc, SNA–AP relation			
Slope, a (mmHg/%)	0.85 ± 0.09	0.86 ± 0.06	0.66 ± 0.10
Intercept, b (mmHg)	37.8 ± 5.2	36.9 ± 5.5	68.0 ± 10.6**,††
AP at 100% SNA (mmHg)	122.7 ± 9.9	122.7 ± 7.0	134.4 ± 4.9
Operating point			
AP (mmHg)	111.4 ± 5.0	110.3 ± 5.1	128.1 ± 4.4**,††
SNA (%)	90.6 ± 7.4	85.8 ± 2.1	94.3 ± 5.9

Data are mean and SE values

CSP Carotid sinus pressure, *AP* arterial pressure, *HR* heart rate, *SNA* sympathetic nerve activity

* $P < 0.05$ and ** $P < 0.01$ from control 1, † $P < 0.05$ and †† $P < 0.01$ from control 2

CSP, however, the baroreflex should be able to control SNA in the presence of ANG II (Fig. 3a). Lumbers et al. [29] pointed out a problem regarding the use of ANG II-induced hypertension as an input perturbation to evaluate the baroreflex.

Effects of ANG II on the baroreflex peripheral arc

The open-loop system characteristics of the baroreflex peripheral arc, assessed using the AP response as a function of SNA, approximated a straight line under both control and ANG II-treated conditions (Fig. 3b), suggesting that the splanchnic SNA may represent changes in systemic SNA that controlled the AP. ANG II significantly increased the intercept of the regression line, reflecting its direct vasoconstrictive effect (Table 1). Because the AP at 100% SNA did not differ among the three conditions, the slope could be shallower in the presence of ANG II. In other words, ANG II appears to elevate the AP to a greater extent for the lower SNA range. Although both the modulation of sympathetic neurotransmission and direct vasoconstriction contribute to the elevation of AP, the fact that ANG II enhances the sympathetic neurotransmission more with a lower stimulation frequency [30, 31] may, in part, account for the greater ANG II-induced increase in AP for the lower SNA range.

Effects of ANG II on the open-loop sympathetic baroreflex control of HR

The baroreflex control of HR showed changes similar to those observed for SNA. Intravenous ANG II increased both the minimum and maximum HR while not significantly affecting the response range of HR or the maximum slope of the response (Fig. 2b; Table 1). The midpoint in CSP was not changed by ANG II. Therefore, the open-loop baroreflex control of HR shifted upward to higher HR values without a concomitant rightward shift to higher CSP values in the present study. In contrast, previous studies reported a rightward shift in the baroreflex control of HR toward higher input pressure values during acute [11, 32] and chronic [33] administration of ANG II in conscious rabbits. Reid and Chou [32] indicated that the inhibition of vagal tone to the heart played a significant role in resetting the baroreflex control of HR in conscious rabbits. It is likely that the rightward shift in the baroreflex control of

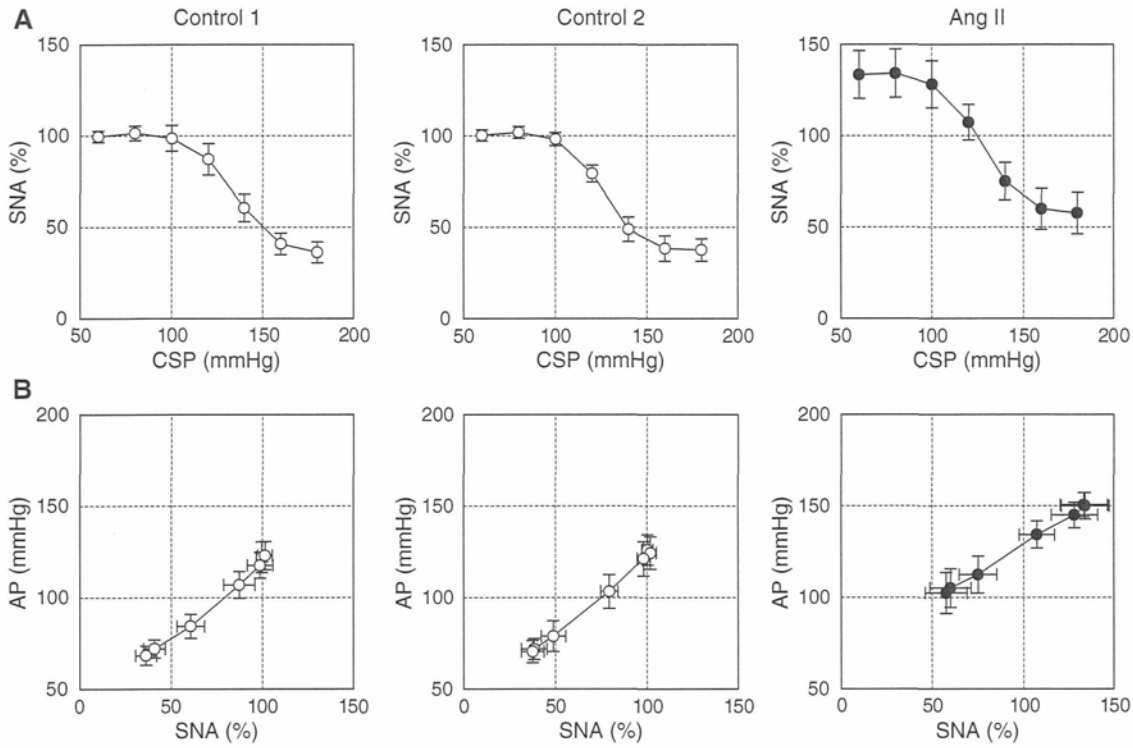

Fig. 3 **a** Averaged input–output relation of the baroreflex neural arc or the arterial baroreflex control of SNA. SNA decreased in response to an increase in the CSP. ANG II increased SNA, while the range of the SNA response was preserved. **b** Averaged input–output relation of the baroreflex peripheral arc. AP increased in response to an increase in SNA. ANG II increased the AP, an effect that was greater for lower SNA

HR by ANG II was not observed in the present study because the vagal nerves were sectioned.

Limitations

First, we performed the experiments in anesthetized animals, and comparisons with results obtained in conscious animals should be made carefully. Circulating levels of ANG II may vary under anesthesia, which could have affected the present results. For instance, reported plasma ANG II concentration in pithed rats is approximately 400 pg/ml [16], which exceeds the plasma ANG II concentration reported in rats with heart failure [34]. Second, although the dose of ANG II used in the present study was within or below those used in previous studies in rats [12, 16, 17], Brown et al. demonstrated that intravenous ANG II at 20 and 270 ng kg^{-1} min^{-1} increased the plasma ANG II concentration from approximately 80 pg/ml to 140 and 2,000 pg/ml, respectively [35]. Based on those data, the plasma ANG II concentration might have been increased beyond a physiologically relevant range to approximately 1,200 pg/ml in the present study. Therefore, the observed effect of ANG II on the arterial baroreflex should be interpreted as pharmacologic. Effects of circulating ANG II can be different when examined in different doses. Third, there was large variation in HR values among the animals (Fig. 2b). Increasing the number of animals would reduce this variation. Nevertheless, data from the eight rats was sufficient to perform statistical analyses and draw reasonable conclusions. Fourth, we occluded the common carotid arteries to isolate the carotid sinuses. Although the vertebral arteries were kept intact and the effects of ANG II were examined using the same preparation, the possibility cannot be ruled out that the carotid occlusion affected the present results. Finally, we cut the vagal nerves to obtain the open-loop condition for the carotid sinus baroreflex. Further studies are needed to clarify the effects of ANG II on the baroreflex control of the cardiovascular system through the vagal system.

Conclusion

The present study indicates that high circulating levels of ANG II significantly increased splanchnic SNA but did not acutely attenuate the range of arterial baroreflex control of SNA. The ranges of the total baroreflex response and the baroreflex control of HR were also preserved during ANG

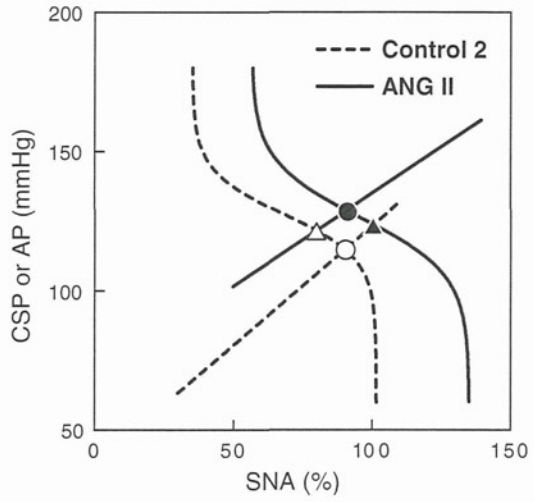

Fig. 4 Equilibrium diagrams between the arterial baroreflex neural and peripheral arcs. The *dashed* and *solid curves* represent the open-loop characteristics of the baroreflex neural arc under the control and ANG II-treated conditions, respectively. The *dashed* and *solid lines* represent the open-loop characteristics of the baroreflex peripheral arc under the control and ANG II-treated conditions, respectively. The *open circle* indicates the closed-loop operating point under the control condition. ANG II causes an upward shift in the peripheral arc. If ANG II does not affect the neural arc, the closed-loop operating point would be at the point depicted by the *open triangle*. In this case, the estimation of baroreflex control of SNA based on the closed-loop operating points (the *open circle* and *open triangle*) approximates the slope of the baroreflex neural arc (*dashed curve*). ANG II, however, causes a rightward shift in the neural arc. Thus, the estimation of the baroreflex control of SNA based on closed-loop operating points (the *open* and *filled circles*) does not match the slope of the neural arc under either the control (*dashed curve*) or ANG II-treated condition (*solid curve*)

II administration. ANG II does modify the arterial baroreflex in that it increases SNA at a given baroreceptor pressure level but does not appear to attenuate the range of arterial baroreflex control of SNA, HR or AP.

Acknowledgments This study was supported by Health and Labour Sciences Research Grants (H18-nano-Ippan-003, H19-nano-Ippan-009, H20-katsudo-Shitei-007, and H21-nano-Ippan-005) from the Ministry of Health, Labour and Welfare of Japan; by a Grant-in-Aid for Scientific Research (No. 20390462) from the Ministry of Education, Culture, Sports, Science and Technology of Japan; and by the Industrial Technology Research Grant Program from the New Energy and Industrial Technology Development Organization (NEDO) of Japan.

References

1. Ikeda Y, Kawada T, Sugimachi M, Kawaguchi O, Shishido T, Sato T, Miyano H, Matsuura W, Alexander J Jr, Sunagawa K (1996) Neural arc of baroreflex optimizes dynamic pressure regulation in achieving both stability and quickness. Am J Physiol 271:H882–H890
2. Kawada T, Yamamoto K, Kamiya A, Ariumi H, Michikami D, Shishido T, Sunagawa K, Sugimachi M (2005) Dynamic characteristics of carotid sinus pressure-nerve activity transduction in rabbits. Jpn J Physiol 55:157–163
3. Sato T, Kawada T, Shishido T, Miyano H, Inagaki M, Miyashita H, Sugimachi M, Kneupfer MM, Sunagawa K (1998) Dynamic transduction properties of in situ baroreceptors of rabbit aortic depressor nerve. Am J Physiol Heart Circ Physiol 274:H358–H365
4. Chapleau MW, Abboud FM (1987) Contrasting effects of static and pulsatile pressure on carotid baroreceptor activity in dogs. Circ Res 61:648–658
5. Kawada T, Fujiki N, Hosomi H (1992) Systems analysis of the carotid sinus baroreflex system using a sum-of-sinusoidal input. Jpn J Physiol 42:15–34
6. Kawada T, Yanagiya Y, Uemura K, Miyamoto T, Zheng C, Li M, Sugimachi M, Sunagawa K (2002) Input-size dependence of the baroreflex neural arc transfer characteristics. Am J Physiol Heart Circ Physiol 284:H404–H415
7. Kawada T, Zheng C, Yanagiya Y, Uemura K, Miyamoto T, Inagaki M, Shishido T, Sugimachi M, Sunagawa K (2002) High-cut characteristics of the baroreflex neural arc preserve baroreflex gain against pulsatile pressure. Am J Physiol Heart Circ Physiol 282:H1149–H1156
8. Reid IA (1992) Interactions between ANG II, sympathetic nervous system, and baroreceptor reflexes in regulation of blood pressure. Am J Physiol Endocrinol Metab 262:E763–E778
9. Sanderford MG, Bishop VS (2000) Angiotensin II acutely attenuates range of arterial baroreflex control of renal sympathetic nerve activity. Am J Physiol Heart Circ Physiol 279:H1804–H1812
10. McMullan S, Goodchild AK, Pilowsky PM (2007) Circulating angiotensin II attenuates the sympathetic baroreflex by reducing the barosensitivity of medullary cardiovascular neurons in the rat. J Physiol 582:711–722
11. Kumagai K, Reid IA (1994) Angiotensin II exerts differential actions on renal nerve activity and heart rate. Hypertension 24:451–456
12. Tan PS, Killinger S, Horiuchi J, Dampney RA (2007) Baroreceptor reflex modulation by circulating angiotensin II is mediated by AT_1 receptors in the nucleus tractus solitarius. Am J Physiol Regul Integr Comp Physiol 293:R2267–R2278
13. Zucker IH (2006) Novel mechanisms of sympathetic regulation in chronic heart failure. Hypertension 48:1005–1011
14. Shoukas AA, Callahan CA, Lash JM, Haase EB (1991) New technique to completely isolate carotid sinus baroreceptor regions in rats. Am J Physiol Heart Circ Physiol 260:H300–H303
15. Sato T, Kawada T, Miyano H, Shishido T, Inagaki M, Yoshimura R, Tatewaki T, Sugimachi M, Alexander J Jr, Sunagawa K (1999) New simple methods for isolating baroreceptor regions of carotid sinus and aortic depressor nerves in rats. Am J Physiol Heart Circ Physiol 276:H326–H332
16. Grant TL, McGrath JC (1988) Interactions between angiotensin II, sympathetic nerve-mediated pressor response and cyclo-oxygenase products in the pithed rat. Br J Pharmacol 95:1220–1228
17. Haywood JR, Fink GD, Buggy J, Phillips MI, Brody MJ (1980) The area postrema plays no role in the pressor action of angiotensin in the rat. Am J Physiol Heart Circ Physiol 239:H108–H113
18. Kent BB, Drane JW, Blumenstein B, Manning JW (1972) A mathematical model to assess changes in the baroreceptor reflex. Cardiology 57:295–310
19. Glantz SA (2002) Primer of biostatistics, 5th edn. McGraw-Hill, New York
20. Mohrman DE, Heller LJ (2006) Cardiovascular physiology, 6th edn. McGraw Hill, New York, pp 172–177
21. Sato T, Kawada T, Inagaki M, Shishido T, Takaki H, Sugimachi M, Sunagawa K (1999) New analytic framework for

understanding sympathetic baroreflex control of arterial pressure. Am J Physiol Heart Circ Physiol 276:H2251–H2261
22. Kawada T, Shishido T, Inagaki M, Zheng C, Yanagiya Y, Uemura K, Sugimachi M, Sunagawa K (2002) Estimation of baroreflex gain using a baroreflex equilibrium diagram. Jpn J Physiol 52:21–29
23. Kashihara K, Takahashi Y, Chatani K, Kawada T, Zheng C, Li M, Sugimachi M, Sunagawa K (2003) Intravenous angiotensin II does not affect dynamic baroreflex characteristics of the neural or peripheral arc. Jpn J Physiol 53:135–143
24. Sanderford MG, Bishop VS (2002) Central mechanisms of acute ANG II modulation of arterial baroreflex control of renal sympathetic nerve activity. Am J Physiol Heart Circ Physiol 282:H1592–H1602
25. Fukiyama K (1972) Central action of angiotensin and hypertension—increased central vasomotor outflow by angiotensin. Jpn Circ J 36:599–602
26. Guo GB, Abboud FM (1984) Angiotensin II attenuates baroreflex control of heart rate and sympathetic activity. Am J Physiol Heart Circ Physiol 246:H80–H89
27. Kamiya A, Kawada T, Yamamoto K, Michikami D, Ariumi H, Uemura K, Zheng C, Shimizu S, Aiba T, Miyamoto T, Sugimachi M, Sunagawa K (2005) Resetting of the arterial baroreflex increases orthostatic sympathetic activation and prevents postural hypotension in rabbits. J Physiol 566:237–246
28. Yamamoto K, Kawada T, Kamiya A, Takaki H, Miyamoto T, Sugimachi M, Sunagawa K (2004) Muscle mechanoreflex induces the pressor response by resetting the arterial baroreflex neural arc. Am J Physiol Heart Circ Physiol 286:H1382–H1388
29. Lumbers ER, McCloskey DI, Potter EK (1979) Inhibition by angiotensin II of baroreceptor-evoked activity in cardiac vagal efferent nerves in the dog. J Physiol 294:69–80
30. Hughes J, Roth RH (1971) Evidence that angiotensin enhances transmitter release during sympathetic nerve stimulation. Br J Phrmacol 41:239–255
31. Zimmerman BG, Gomer SK, Liao JC (1972) Action of angiotensin on vascular adrenergic nerve endings: facilitation of norepinephrine release. Federation Proc 31:1344–1350
32. Reid IA, Chou L (1990) Analysis of the action of angiotensin II on the baroreflex control of heart rate in conscious rabbits. Endocrinology 126:2749–2756
33. Brooks VL (1995) Chronic infusion of angiotensin II resets baroreflex control of heart rate by an arterial pressure-independent mechanism. Hypertension 26:420–424
34. Schunkert H, Tang SS, Litwin SE, Diamant D, Riegger G, Dzau VJ, Ingelfinger JR (1993) Regulation of intrarenal and circulating renin–angiotensin systems in severe heart failure in the rat. Cardiovasc Res 27:731–735
35. Brown AJ, Casals-Stenzel J, Gofford S, Lever AF, Morton JJ (1981) Comparison of fast and slow pressor effects of angiotensin II in the conscious rat. Am J Physiol Heart Circ Physiol 241:H381–H388

Life Sciences 85 (2009) 597–601

Contents lists available at ScienceDirect

Life Sciences

journal homepage: www.elsevier.com/locate/lifescie

Detection of endogenous acetylcholine release during brief ischemia in the rabbit ventricle: A possible trigger for ischemic preconditioning

Toru Kawada [a,*], Tsuyoshi Akiyama [b], Shuji Shimizu [a], Atsunori Kamiya [a], Kazunori Uemura [a], Meihua Li [a], Mikiyasu Shirai [b], Masaru Sugimachi [a]

[a] Department of Cardiovascular Dynamics, Advanced Medical Engineering Center, National Cardiovascular Center Research Institute, Japan
[b] Department of Cardiac Physiology, National Cardiovascular Center Research Institute, Japan

ARTICLE INFO

Article history:
Received 1 July 2009
Accepted 25 August 2009

Keywords:
Acetylcholine
Cardiac microdialysis
Vagal stimulation
Coronary artery occlusion
Rabbits

ABSTRACT

Aims: To examine endogenous acetylcholine (ACh) release in the rabbit left ventricle during acute ischemia, ischemic preconditioning and electrical vagal stimulation.
Main methods: We measured myocardial interstitial ACh levels in the rabbit left ventricle using a cardiac microdialysis technique. In Protocol 1 ($n=6$), the left circumflex coronary artery (LCX) was occluded for 30 min and reperfused for 30 min. In Protocol 2 ($n=5$), the LCX was temporarily occluded for 5 min. Ten minutes later, the LCX was occluded for 30 min and reperfused for 30 min. In Protocol 3 ($n=5$), bilateral efferent vagal nerves were stimulated at 20 Hz and 40 Hz (10 V, 1-ms pulse duration).
Key findings: In Protocol 1, a 30-min coronary occlusion increased the ACh level from 0.39 ± 0.15 to 7.0 ± 2.2 nM (mean ± SE, $P<0.01$). In Protocol 2, a 5-min coronary occlusion increased the ACh level from 0.33 ± 0.07 to 0.75 ± 0.11 nM ($P<0.05$). The ACh level returned to 0.48 ± 0.10 nM during the interval. After that, a 30-min coronary occlusion increased the ACh level to 2.4 ± 0.49 nM ($P<0.01$). In Protocol 3, vagal stimulation at 20 Hz and 40 Hz increased the ACh level from 0.29 ± 0.06 to 1.23 ± 0.48 ($P<0.05$) and 2.44 ± 1.13 nM ($P<0.01$), respectively.
Significance: Acute ischemia significantly increased the ACh levels in the rabbit left ventricle, which appeared to exceed the vagal stimulation-induced ACh release. Brief ischemia as short as 5 min can also increase the ACh level, suggesting that endogenous ACh release can be a trigger for ischemic preconditioning.

Introduction

Although ventricular vagal innervation is sparser than that observed in the atrium, we have previously demonstrated that electrical vagal stimulation and acute myocardial ischemia significantly increased myocardial interstitial acetylcholine (ACh) levels in the feline left ventricle (Kawada et al. 2000, 2001, 2006a,b, 2007). Potential differences between species, however, suggest that data obtained from the feline left ventricle may not be directly extrapolated to ventricular vagal innervation in other species (Brown 1976; Kilbinger and Löffelholz 1976). Compared with the feline heart, the rabbit heart is more frequently analyzed in investigations of myocardial ischemia and ischemic preconditioning. For instance, Qin et al. (2003) used isolated rabbit hearts to demonstrate that ACh and adenosine induce ischemic preconditioning mimetic effects through different signaling pathways. In our previous study, vagal stimulation increased the level of tissue inhibitor of metalloproteinase-1 (TIMP-1) and reduced the level of endogenous active matrix metalloproteinase-9 (MMP-9) during ischemia–reperfusion injury in the rabbit left ventricle (Uemura et al. 2007). Despite its potential cardioprotective effects against myocardial ischemia, the profile of endogenous ACh release in the rabbit left ventricle is poorly understood *in vivo* owing to the difficulty in detecting low levels of myocardial interstitial ACh. Quantification of endogenous ACh release during myocardial ischemia and electrical vagal stimulation would help understand the potential cardioprotective effects of vagal stimulation. In the present study, we examined the effects of acute myocardial ischemia, ischemic preconditioning, and electrical vagal stimulation on myocardial interstitial ACh levels in the rabbit left ventricle *in vivo* using an improved high-performance liquid chromatography (HPLC) system that allowed us to detect low concentrations of ACh (Shimizu et al. 2009).

Materials and methods

Surgical preparation and protocols

Animal care was conducted in accordance with the *Guiding Principles for the Care and Use of Animals in the Field of Physiological Sciences*, which has been approved by the Physiological Society of

* Corresponding author. Department of Cardiovascular Dynamics, Advanced Medical Engineering Center, National Cardiovascular Center Research Institute, 5-7-1 Fujishirodai, Suita, Osaka 565-8565, Japan. Tel.: +81 6 6833 5012x2427; fax: +81 6 6835 5403.
E-mail address: torukawa@res.ncvc.go.jp (T. Kawada).

0024-3205/$ – see front matter © 2009 Published by Elsevier Inc.
doi:10.1016/j.lfs.2009.08.015

Japan. Japanese white rabbits weighing 2.5 kg to 3.1 kg (2.8 ± 0.1 kg, mean ± SE) were anesthetized via intravenous administration of pentobarbital sodium (30–35 mg/kg) through a marginal ear vein. The animals were ventilated mechanically with room air mixed with oxygen. The anesthetic condition was maintained using a continuous intravenous infusion of urethane (125 mg kg^{-1} h^{-1}) and α-chloralose (20 mg kg^{-1} h^{-1}) through a catheter inserted in the right femoral vein. Mean arterial pressure (AP) was measured using a catheter inserted in the right femoral artery. Heart rate (HR) was measured from an electrocardiogram obtained using a cardiotachometer. The animal was placed in a lateral position, and the left fourth and fifth ribs were partially resected to allow access to the heart. The heart was suspended in a pericardial cradle.

In Protocol 1 ($n = 6$), which was designed to examine the effects of acute myocardial ischemia and reperfusion, a 3-0 silk suture was passed around a branch of the left circumflex coronary artery (LCX); both ends were passed through a polyethylene tube to make a snare to occlude the artery. A dialysis probe was implanted into the anterolateral free wall of the left ventricle perfused by the LCX. After collecting a baseline dialysate sample, the LCX was occluded for 30 min and reperfused for 30 min. After the ischemia–reperfusion protocol was finished, the LCX was occluded again and a 5-ml bolus of 1% methylene blue was injected intravenously to confirm that the dialysis probe had been implanted within the area at risk for myocardial ischemia.

In Protocol 2 ($n = 5$), which was designed to examine the effects of ischemic preconditioning (*i.e.*, a brief ischemic event preceding a major ischemic event), a 3-0 silk suture was passed around a branch of the LCX and both ends were passed through a polyethylene tube to make a snare. Two dialysis probes were implanted into the anterolateral free wall of the left ventricle perfused by the LCX; the probes were separated by at least 5 mm. Combining the dialysate samples obtained from the two dialysis probes increased the time resolution of the ACh measurement. After collecting a baseline dialysate sample, the LCX was temporarily occluded for 5 min which was followed by a 10-min interval. The LCX was then occluded for 30 min and reperfused for 30 min. After the ischemia–reperfusion protocol was completed, the LCX was occluded again and a 5-ml bolus of 1% methylene blue was injected intravenously to confirm that the two dialysis probes had been implanted within the area at risk for myocardial ischemia.

In Protocol 3 ($n = 5$), which was designed to examine the effects of electrical vagal stimulation, the vagus nerves were exposed and sectioned at the neck. Each sectioned vagus nerve was placed on a pair of bipolar platinum electrodes to stimulate the efferent vagus nerve. The nerve and the electrodes were fixed using silicone glue (Kwik-Sil, World Precision Instruments, Sarasota, FL, USA). Two dialysis probes were implanted into the anterolateral free wall of the left ventricle; the probes were separated by at least 5 mm. Dialysate samples obtained from the two dialysis probes were analyzed separately. After collecting baseline dialysate samples, the vagus nerves were stimulated at 20 Hz for 15 min and 40 Hz for 15 min. The stimulation amplitude was 10 V and the pulse duration was 1 ms. The 40-Hz stimulation often caused an initial cardiac arrest for a few seconds and was considered to be the most intensive stimulation in the present experimental settings. The 20-Hz stimulation was arbitrarily selected at a half of the maximum stimulation rate to observe the dependence of the ACh release on the stimulation rate.

At the end of each protocol, the experimental animals were sacrificed with an overdose of intravenous pentobarbital sodium. We performed a postmortem examination and confirmed that the dialysis probe(s) had been implanted within the left ventricular myocardium.

Dialysis technique

We measured dialysate concentrations of ACh as indices of myocardial interstitial ACh levels. The materials and properties of the dialysis probe have been described previously (Akiyama et al. 1994). Briefly, we designed a transverse dialysis probe. A dialysis fiber (length, 8 mm; outer diameter, 310 μm; inner diameter, 200 μm; PAN-1200, 50,000-Da molecular-weight cutoff, Asahi Chemical, Japan) was glued at both ends to polyethylene tubes (length, 25 cm; outer diameter, 500 μm; inner diameter, 200 μm). The dialysis probe was perfused at a rate of 2 μl/min with Ringer's solution containing a cholinesterase inhibitor eserine (100 μM). Dialysate sampling was started from 2 h after probe implantation. In Protocols 1 and 3, one sampling period was set at 15 min, which yielded a sample volume of 30 μl. The actual dialysate sampling lagged behind a given collection period by 5 min owing to the dead space volume between the dialysis membrane and collecting tube. In Protocol 2, one sampling period was set at 5 min to increase the time resolution during the ischemic preconditioning, and dialysate samples from the two dialysis probes were combined to yield a sample volume of 20 μl. The sampling period was changed to 10 min during the main ischemic event to reduce the total number of samples. The amount of ACh in the dialysate was measured using an HPLC system with electrochemical detection (Eicom, Japan) adjusted to measure low levels of ACh (Shimizu et al. 2009). The concentration of ACh was calculated taking the sample volume in account.

Statistical analysis

All data are presented as the mean and SE values. We performed repeated-measures analysis of variance, followed by a Tukey test for all pairwise, multiple comparisons to examine changes in the ACh levels (Glantz 2002). Because the variance of measured ACh levels increased with their mean, statistical analysis was performed after logarithmic conversion of the ACh data (Snedecor and Cochran 1989). The AP and HR data were examined using repeated-measures analysis of variance, followed by a Dunnett's test for multiple comparisons against a single control (Glantz 2002). In Protocols 1 and 3, the baseline value was treated as the single control. In Protocol 2, the value measured just before the main ischemic event was treated as the single control. In all of the statistical analyses, differences were considered significant when $P < 0.05$.

Results

In Protocol 1, the myocardial interstitial ACh levels significantly increased during ischemia compared with the baseline value (Fig. 1). Although the ACh levels declined during reperfusion, they were still significantly higher than the baseline value. Changes in AP and HR are summarized in Table 1. Although AP did not change significantly during ischemia, it decreased significantly throughout the reperfusion period. The HR increased significantly after 30 min of ischemia, and remained high during the reperfusion period with the exception of the last data point.

In Protocol 2, the LCX was occluded for 5 min (ischemic preconditioning) and released for 10 min before the major ischemic event. The brief 5-min occlusion significantly increased the myocardial interstitial ACh level compared with the baseline value (Fig. 2). The ACh levels during the interval between the brief occlusion and the major occlusion did not differ from the baseline value. The ACh levels increased significantly during the major ischemic event compared with the baseline value. Although the ACh levels declined during reperfusion, they were still significantly higher than the baseline value. Changes in AP and HR are summarized in Table 2. Neither AP nor HR changed significantly compared with the respective control values measured after the 10-min middle interval.

In Protocol 3, electrical vagal stimulation significantly increased the myocardial interstitial ACh levels (Fig. 3). The ACh levels returned close to the baseline value just after vagal stimulation was terminated. The AP and HR values were significantly reduced by vagal stimulation (Table 3).

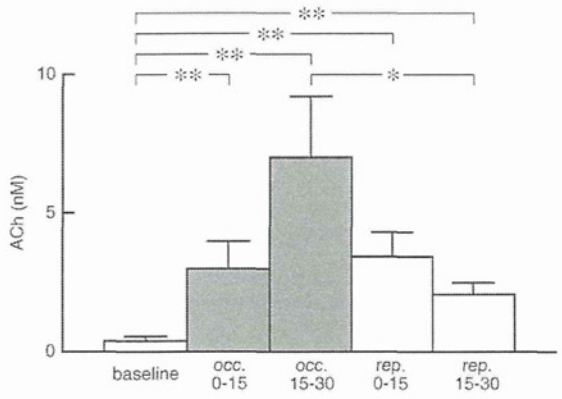

Fig. 1. Changes in the myocardial interstitial ACh levels in Protocol 1. The left circumflex coronary artery was occluded for 30 min and reperfused for 30 min. occ: occlusion; rep: reperfusion. Data are shown as the mean + SE ($n = 6$). *$P < 0.05$ and **$P < 0.01$; Tukey test.

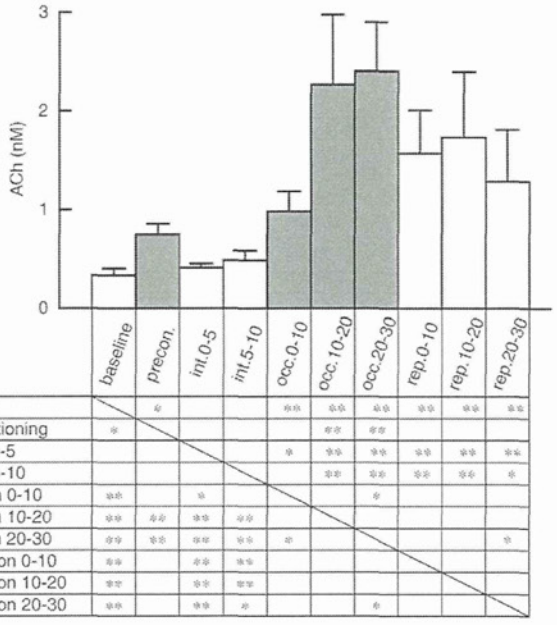

Fig. 2. Changes in the myocardial interstitial ACh levels in Protocol 2. The left circumflex coronary artery was occluded for 5 min. Ten minutes later, the left circumflex coronary artery was occluded for 30 min and reperfused for 30 min. precon: preconditioning; int: interval; occ: occlusion; rep: reperfusion. Data are shown as the mean + SE ($n = 5$). *$P < 0.05$ and **$P < 0.01$; Tukey test.

Discussion

Effects of acute ischemia on myocardial interstitial ACh levels

Acute myocardial ischemia significantly increased myocardial interstitial ACh levels in the ischemic region (Fig. 1). To our knowledge, this is the first report demonstrating ischemia-induced ACh release in the rabbit left ventricle *in vivo*. Because electrical vagal stimulation increased the myocardial interstitial ACh levels (Fig. 3), centrally mediated activation of the efferent vagus nerve could contribute to these effects. LCX occlusion, however, did not decrease the HR significantly (Table 1), suggesting that centrally mediated vagal activation did not have a marked role in the present study. In a previous study, acute myocardial ischemia increased myocardial interstitial ACh levels in vagotomized cats, suggesting an important role of a local release mechanism that is independent of efferent vagal activity (Kawada et al. 2000). Intracellular Ca^{2+} mobilization related to cation-selective stretch-activated channels is thought to be involved in this local release mechanism (Kawada et al. 2000, 2006b). A similar local mechanism may be responsible for ischemia-induced ACh release in the rabbit left ventricle.

In our previous study, topical perfusion of ACh through a dialysis probe increased TIMP-1 levels in the rabbit left ventricle (Uemura et al. 2007). The production of TIMP-1 reduces endogenous levels of active MMP-9, which can limit ventricular remodeling following myocardial ischemia and reperfusion. Whether ischemia-induced ACh release can induce such an anti-remodeling effect remains unanswered, however, because reperfusion reduced the myocardial interstitial ACh levels toward the baseline value. Whether prolonged ischemia for more than 30 min induces sustained elevations of ACh levels is an interesting topic for future studies.

The ACh levels were decreased toward the baseline value upon reperfusion, probably by the washout of ACh from the interstitial fluid. In the case of myocardial interstitial myoglobin levels, the reperfusion further increases the myoglobin levels, suggesting an occurrence of reperfusion injury to the myocardium (Kitagawa et al. 2005). Reoxygenation upon reperfusion rapidly restores the ATP synthesis, which can cause hypercontracture of myofibrils and undesired cytoskeletal lesions (Piper et al. 2004). Because the vagal nerve endings do not have contractile elements, the hypercontracture-induced cell injury does not occur, and the further release of ACh may have been prevented.

Effects of ischemic preconditioning on myocardial interstitial ACh levels

Ischemic preconditioning is a phenomenon in which a brief ischemic event makes the heart resistant to a subsequent ischemic insult (Murry et al. 1986). Acetylcholine, bradykinin, and adenosine are endogenous substances that can induce ischemic preconditioning mimetic effects in the rabbit heart (Liu et al. 1991; Qin et al. 2003; Krieg et al. 2004). In a previous study, we showed that a 5-min ischemic event increased myocardial interstitial ACh levels in the feline ventricle (Kawada et al. 2002). Ischemic preconditioning, however, is not frequently examined in the feline ventricle, making interpretation of these results difficult. In the present study, a 5-min ischemic event caused a significant increase in the ACh level in the rabbit left ventricle (Fig. 2), suggesting that brief ischemia-induced ACh release may serve as a trigger for the ischemic preconditioning. Krieg et al. (2004) demonstrated that ACh triggers preconditioning by sequentially activating Akt and nitric oxide synthase to produce reactive oxygen species. An acetylcholine-induced preconditioning mimetic effect has also been observed in canine (Yao and Gross 1993; Przyklenk and Kloner 1995) and rat (Richard et al. 1995) models.

Table 1
Mean arterial pressure (AP) and heart rate (HR) obtained during Protocol 1 ($n = 6$).

	Baseline	Occlusion 5 min	Occlusion 15 min	Occlusion 30 min	Reperfusion 5 min	Reperfusion 15 min	Reperfusion 30 min
AP(mm Hg)	82 ± 4	77 ± 4	72 ± 5	75 ± 5	72 ± 5*	70 ± 4*	70 ± 2**
HR (beats/min)	247 ± 16	264 ± 14	265 ± 13	280 ± 10**	278 ± 9*	277 ± 8*	274 ± 9

Data are shown as the mean ± SE. *$P < 0.05$ and **$P < 0.01$ vs. baseline using Dunnett's test.

Table 2
Mean arterial pressure (AP) and heart rate (HR) obtained during Protocol 2 ($n=5$).

	Baseline	Preconditioning 5 min	Interval 5 min	Interval 10 min	Occlusion 5 min	Occlusion 10 min
AP(mm Hg)	83±5	77±5	78±4	80±4	78±5	78±5
HR(beats/min)	277±7	282±8	282±7	284±5	285±5	286±6
	Occlusion 20 min	Occlusion 30 min	Reperfusion 5 min	Reperfusion 10 min	Reperfusion 20 min	Reperfusion 30 min
AP(mm Hg)	77±4	78±5	77±5	78±5	77±3	79±3
HR(beats/min)	287±5	289±6	290±5	289±5	290±6	293±5

Data are shown as the mean±SE. No significant differences relative to control values (the value 10 min after the preconditioning) were observed based on Dunnett's test.

In a previous study examining the feline ventricle (Kawada et al. 2002), brief ischemia significantly decreased the HR, highlighting the presence of a significant vagal reflex from the heart. Vagotomy abolished the ACh release induced by brief ischemia in that study, suggesting an important role of centrally mediated vagal activation. The vagal reflex from the heart, however, shows regional differences and varies among species (Thames et al. 1978; Kawada et al. 2007). In the present study, brief ischemia did not decrease the HR significantly (Table 2), suggesting that centrally mediated vagal activation was not a major factor for the brief ischemia-induced ACh release in the rabbit heart.

Rabbits exhibit marked effects from ischemic preconditioning, including reduced infarct size (Cohen et al. 1991; Cason et al. 1997). Although whether the ACh release induced by the brief ischemic event exerted cardioprotective effects was not examined in the present study, there was a notable difference in the changes in AP observed with Protocol 1 and Protocol 2. Although AP decreased significantly upon reperfusion in Protocol 1 (Table 1), it did not change significantly during the major ischemic event in Protocol 2 (Table 2), possibly reflecting preserved cardiac function as a result of the ischemic preconditioning.

Effects of electrical vagal stimulation on myocardial interstitial ACh levels

In the feline left ventricle, electrical vagal stimulation at 20 Hz (10 V, 1-ms pulse duration) increases myocardial interstitial ACh levels to approximately 20 nM as measured with a dialysis fiber 13 mm in length (Kawada et al. 2000). In contrast, electrical vagal stimulation at 20 Hz in the rabbit left ventricle (10 V, 1-ms pulse duration) increased the ACh levels to approximately 1.2 nM as measured with a dialysis fiber 8 mm long (Fig. 3). The small increase in the ACh level detected during electrical vagal stimulation may indicate that vagal innervation is much sparser in the rabbit ventricle

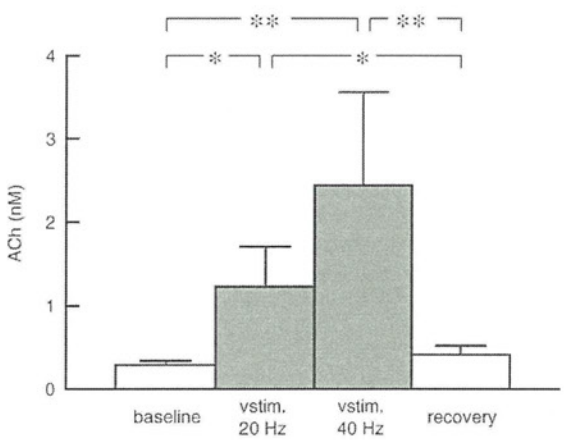

Fig. 3. Changes in the myocardial interstitial ACh levels in Protocol 3. The bilateral efferent vagus nerves were stimulated at 20 Hz for 15 min and 40 Hz for 15 min. Data are shown as the mean + SE ($n=10$, 2 samples from each of the 5 animals). *$P<0.05$ and **$P<0.01$; Tukey test.

than in the feline ventricle. In a previous study that used a dialysis fiber 4 mm in length, right vagal stimulation at 20 Hz increased the dialysate ACh concentration from 0.4±0.2 nM to 0.9±0.3 nM, whereas left vagal stimulation at 20 Hz increased it from 0.3±0.1 nM to 1.0±0.4 nM in the rabbit right ventricle (Shimizu et al. 2009). Considering the bilateral stimulation and fiber length of 8 mm in the present study, the vagal innervation of the left ventricle may be comparable to or slightly sparser than that of the right ventricle.

The dialysis fiber differed in length among studies due to anatomical restrictions related to the fiber implantation procedure (*i.e.*, size of the heart etc.). If we consider diffusive processes alone, the relative recovery (RR) can be expressed as:

$$RR = \frac{C_{\text{inside}}}{C_{\text{outside}}} = 1 - \exp\left(-k\frac{A}{F}\right) = 1 - \exp\left(-k\frac{mL}{F}\right)$$

where C_{inside} and C_{outside} are the ACh concentrations inside and outside the dialysis fiber; A is the surface area of the dialysis membrane, which can be proportional to the fiber length L with a coefficient m; F is a perfusion flow rate; and k is the mass transfer coefficient (Ståhle 1991). The *in vitro* RR for ACh is approximately 70% with $F=2$ µl/min and $L=13$ mm (Akiyama et al. 1994), which yields $km=0.1852$. Using this value, the *in vitro* RR would be approximately 52% for $L=8$ mm and 31% for $L=4$ mm. Although these values provide some clues to speculate the effects of fiber length on the detected ACh concentrations, they cannot be directly extrapolated to the present results, because k should be different in *in vivo* conditions.

The physiological significance of vagal innervation of the left ventricle is controversial, because fixed-rate atrial pacing abolishes vagally induced inhibition of left ventricular contractility in an experimental setting without significant background sympathetic tone (Matsuura et al. 1997). On the other hand, when the cardiac sympathetic nerve is activated, vagal stimulation can reduce ventricular contractility even under fixed-rate atrial pacing by antagonizing the sympathetic effect (Nakayama et al. 2001). In addition, vagal stimulation suppresses myocardial interstitial myoglobin release during acute myocardial ischemia in anesthetized cats (Kawada et al. 2008). Chronic vagal stimulation improves the survival rate of rat models of chronic heart failure after myocardial infarction (Li et al. 2004). These lines of evidence suggest that vagal innervation of the left ventricle may be of therapeutic significance.

An unresolved question regarding the cardioprotective effects of vagal stimulation is that a large quantity of ACh is released in the ischemic region without vagal stimulation (Fig. 1). In the present

Table 3
Mean arterial pressure (AP) and heart rate (HR) obtained during Protocol 3 ($n=5$).

	Baseline	Vagal stimulation 20 Hz	Vagal stimulation 40 Hz	Recovery
AP (mm Hg)	100±3	59±9**	54±9**	86±5
HR (beats/min)	322±14	126±5**	100±8**	311±8

Data are shown as the mean±SE. **$P<0.01$ vs. baseline based on Dunnett's test.

study, vagal stimulation at 20-Hz lowered the HR by approximately 200 beats/min (to less than 40% of the control value) but the stimulation-induced ACh release did not exceed the ischemia-induced ACh release (Figs. 1 and 3). On the other hand, vagal stimulation that reduced the HR by only 10% produces a significant increase in the survival rate of chronic heart failure rats (Li et al. 2004). Therefore, vagal stimulation probably exerts its beneficial effects not only within the ischemic region but also outside of this region. For instance, vagal stimulation in dogs with a healed myocardial infarction is known to prevent lethal arrhythmia induced by exercise (Vanoli et al. 1991). Afferent vagal activation may also contribute to the cardioprotective effects. Further studies are clearly needed to identify the mechanisms underlying the vagally induced cardioprotective effects against myocardial infarction and chronic heart failure.

Conclusion

The present study demonstrated the presence of vagal innervation in the rabbit left ventricle. Acute myocardial ischemia significantly increased the myocardial interstitial ACh levels. In addition, a brief ischemic event (5 min) caused detectable increases in ACh levels, indicating that endogenous ACh release may provide a trigger for ischemic preconditioning.

Acknowledgments

This study was supported by the Health and Labour Sciences Research Grants (H18-nano-Ippan-003, H19-nano-Ippan-009, H20-katsudo-Shitei-007, and H21-nano-Ippan-005) from the Ministry of Health, Labour and Welfare of Japan; by a Grant-in-Aid for Scientific Research (No. 20390462) from the Ministry of Education, Culture, Sports, Science and Technology of Japan; and by the Industrial Technology Research Grant Program from the New Energy and Industrial Technology Development Organization (NEDO) of Japan.

References

Akiyama T, Yamazaki T, Ninomiya I. In vivo detection of endogenous acetylcholine release in cat ventricles. American Journal of Physiology 266 (3 Pt 2), H854–H860, 1994.

Brown OM. Cat heart acetylcholine: Structural proof and distribution. American Journal of Physiology 231 (3), 781–785, 1976.

Cason BA, Gamperl AK, Slocum RE, Hickey RF. Anesthetic-induced preconditioning: Previous administration of isoflurane decreases myocardial infarct size in rabbits. Anesthesiology 87 (5), 1182–1190, 1997.

Cohen MV, Liu GS, Downey JM. Preconditioning causes improved wall motion as well as smaller infarcts after transient coronary occlusion in rabbits. Circulation 84 (1), 341–349, 1991.

Glantz SA. Primer of Biostatistics, 5th ed. McGraw-Hill, New York, 2002.

Kawada T, Yamazaki T, Akiyama T, Sato T, Shishido T, Inagaki M, Takaki H, Sugimachi M, Sunagawa K. Differential acetylcholine release mechanisms in the ischemic and non-ischemic myocardium. Journal of Molecular and Cellular Cardiology 32 (3), 405–414, 2000.

Kawada T, Yamazaki T, Akiyama T, Shishido T, Inagaki M, Uemura K, Miyamoto T, Sugimachi M, Takaki H, Sunagawa K. In vivo assessment of acetylcholine releasing function at cardiac vagal nerve terminals. American Journal of Physiology. Heart and Circulatory Physiology 281 (1), H139–H145, 2001.

Kawada T, Yamazaki T, Akiyama T, Mori H, Inagaki M, Shishido T, Takaki H, Sugimachi M, Sunagawa K. Effects of brief ischaemia on myocardial acetylcholine and noradrenaline levels in anaesthetized cats. Autonomic Neuroscience: Basic and Clinical 95 (1–2), 37–42, 2002.

Kawada T, Yamazaki T, Akiyama T, Li M, Ariumi H, Mori H, Sunagawa K, Sugimachi M. Vagal stimulation suppresses ischemia-induced myocardial interstitial norepinephrine release. Life Sciences 78 (8), 882–887, 2006a.

Kawada T, Yamazaki T, Akiyama T, Uemura K, Kamiya A, Shishido T, Mori H, Sugimachi M. Effects of Ca^{2+} channel antagonists on nerve stimulation-induced and ischemia-induced myocardial interstitial acetylcholine release in cats. American Journal of Physiology. Heart and Circulatory Physiology 291 (5), H2187–H2191, 2006b.

Kawada T, Yamazaki T, Akiyama T, Shishido T, Shimizu S, Mizuno M, Mori H, Sugimachi M. Regional difference in ischaemia-induced myocardial interstitial noradrenaline and acetylcholine releases. Autonomic Neuroscience: Basic and Clinical 137 (1–2), 44–50, 2007.

Kawada T, Yamazaki T, Akiyama T, Kitagawa H, Shimizu S, Mizuno M, Li M, Sugimachi M. Vagal stimulation suppresses ischemia-induced myocardial interstitial myoglobin release. Life Sciences 83 (13–14), 490–495, 2008.

Kilbinger H, Löffelholz K. The isolated perfused chicken heart as a tool for studying acetylcholine output in the absence of cholinesterase inhibition. Journal of Neural Transmission 38, 9–14, 1976.

Kitagawa H, Yamazaki T, Akiyama T, Sugimachi M, Sunagawa K, Mori H. Microdialysis separately monitors myocardial interstitial myoglobin during ischemia and reperfusion. American Journal of Physiology Heart and Circulatory Physiology 289 (2), H924–H930, 2005.

Krieg T, Qin Q, Philipp S, Alexeyev MF, Cohen MV, Downey JM. Acetylcholine and bradykinin trigger preconditioning in the heart through a pathway that induces Akt and NOS. American Journal of Physiology. Heart and Circulatory Physiology 287 (6), H2606–H2611, 2004.

Li M, Zheng C, Sato T, Kawada T, Sugimachi M, Sunagawa K. Vagal nerve stimulation markedly improves long-term survival after chronic heart failure in rats. Circulation 109 (1), 120–124, 2004.

Liu GS, Thornton J, Van Winkle DM, Stanley AW, Olsson RA, Downey JM. Protection against infarction afforded by preconditioning is mediated by A_1 adenosine receptors in rabbit heart. Circulation 84 (1), 350–356, 1991.

Matsuura W, Sugimachi M, Kawada T, Sato T, Shishido T, Miyano H, Nakahara T, Ikeda Y, Alexander Jr J, Sunagawa K. Vagal stimulation decreases left ventricular contractility mainly through negative chronotropic effect. American Journal of Physiology 273 (2 Pt 2), H534–H539, 1997.

Murry CE, Jennings RB, Reimer KA. Preconditioning with ischemia: A delay of lethal cell injury in ischemic myocardium. Circulation 74 (5), 1124–1136, 1986.

Nakayama Y, Miyano H, Shishido T, Inagaki M, Kawada T, Sugimachi M, Sunagawa K. Heart rate-independent vagal effect on end-systolic elastance of the canine left ventricle under various levels of sympathetic tone. Circulation 104 (19), 2277–2279, 2001.

Piper HM, Abdallah Y, Schäfer C. The first minutes of reperfusion: A window of opportunity for cardioprotection. Cardiovascular Research 61 (3), 365–371, 2004.

Przyklenk K, Kloner RA. Low-dose iv acetylcholine acts as a "preconditioning-mimetic" in the canine model. Journal of Cardiac Surgery 10 (4), 389–395, 1995.

Qin Q, Downey JM, Cohen MV. Acetylcholine but not adenosine triggers preconditioning through PI3-kinase and a tyrosine kinase. American Journal of Physiology. Heart and Circulatory Physiology 284 (2), H727–H734, 2003.

Richard V, Blanc T, Kaeffer N, Tron C, Thuillez C. Myocardial and coronary endothelial protective effects of acetylcholine after myocardial ischaemia and reperfusion in rats: Role of nitric oxide. British Journal of Pharmacology 115 (8), 1532–1538, 1995.

Shimizu S, Akiyama T, Kawada T, Shishido T, Yamazaki T, Kamiya A, Mizuno M, Sano S, Sugimachi M. In vivo direct monitoring of vagal acetylcholine release to the sinoatrial node. Autonomic Neuroscience: Basic and Clinical 148 (1–2), 44–49, 2009.

Snedecor GW, Cochran WG. Statistical Methods. Iowa State, Iowa, pp. 290–291, 1989.

Ståhle L. The use of microdialysis in pharmacokinetics and pharmacodynamics. In: Robinson, TE, JusticeJr. Jr, JB (Eds.), Microdialysis in the Neurosciences, pp. 155–174. Elsevier Science Ltd. New York, 1991.

Thames MD, Klopfenstein HS, Abboud FM, Mark AL, Walker JL. Preferential distribution of inhibitory cardiac receptors with vagal afferents to the inferoposterior wall of the left ventricle activated during coronary occlusion in the dog. Circulation Research 43 (4), 512–519, 1978.

Uemura K, Li M, Tsutsumi T, Yamazaki T, Kawada T, Kamiya A, Inagaki M, Sunagawa K, Sugimachi M. Efferent vagal nerve stimulation induces tissue inhibitor of metalloproteinase-1 in myocardial ischemia–reperfusion injury in rabbit. American Journal of Physiology. Heart and Circulatory Physiology 293 (4), H2254–H2261, 2007.

Vanoli E, de Ferrari GM, Stramba-Badiale M, Hull Jr SS, Foreman RD, Schwartz PJ. Vagal stimulation and prevention of sudden death in conscious dogs with a healed myocardial infarction. Circulation Research 68 (5), 1471–1481, 1991.

Yao Z, Gross GJ. Acetylcholine mimics ischemic preconditioning via a glibenclamide-sensitive mechanism in dogs. American Journal of Physiology 264 (6 Pt 2), H2221–H2225, 1993.

Metformin Prevents Progression of Heart Failure in Dogs
Role of AMP-Activated Protein Kinase

Hideyuki Sasaki, MD; Hiroshi Asanuma, MD, PhD; Masashi Fujita, MD, PhD; Hiroyuki Takahama, MD, PhD; Masakatsu Wakeno, MD, PhD; Shin Ito, MD; Akiko Ogai, BS; Masanori Asakura, MD, PhD; Jiyoong Kim, MD; Tetsuo Minamino, MD, PhD; Seiji Takashima, MD, PhD; Shoji Sanada, MD, PhD; Masaru Sugimachi, MD, PhD; Kazuo Komamura, MD, PhD; Naoki Mochizuki, MD, PhD; Masafumi Kitakaze, MD, PhD

Background—Some studies have shown that metformin activates AMP-activated protein kinase (AMPK) and has a potent cardioprotective effect against ischemia/reperfusion injury. Because AMPK also is activated in animal models of heart failure, we investigated whether metformin decreases cardiomyocyte apoptosis and attenuates the progression of heart failure in dogs.

Methods and Results—Treatment with metformin (10 μmol/L) protected cultured cardiomyocytes from cell death during exposure to H_2O_2 (50 μmol/L) via AMPK activation, as shown by the MTT assay, terminal deoxynucleotidyl transferase–mediated dUTP nick-end labeling staining, and flow cytometry. Continuous rapid ventricular pacing (230 bpm for 4 weeks) caused typical heart failure in dogs. Both left ventricular fractional shortening and left ventricular end-diastolic pressure were significantly improved in dogs treated with oral metformin at 100 $mg \cdot kg^{-1} \cdot d^{-1}$ (n=8) (18.6±1.8% and 11.8±1.1 mm Hg, respectively) compared with dogs receiving vehicle (n=8) (9.6±0.7% and 22±0.9 mm Hg, respectively). Metformin also promoted phosphorylation of both AMPK and endothelial nitric oxide synthase, increased plasma nitric oxide levels, and improved insulin resistance. As a result of these effects, metformin decreased apoptosis and improved cardiac function in failing canine hearts. Interestingly, another AMPK activator (AICAR) had effects equivalent to those of metformin, suggesting the primary role of AMPK activation in reducing apoptosis and preventing heart failure.

Conclusions—Metformin attenuated oxidative stress–induced cardiomyocyte apoptosis and prevented the progression of heart failure in dogs, along with activation of AMPK. Therefore, metformin may be a potential new therapy for heart failure. (***Circulation.*** **2009;119:2568-2577.)**

Key Words: AMP-activated protein kinase ■ heart failure ■ metformin ■ nitric oxide

Metformin is widely used as an antidiabetic drug with an insulin-sensitizing effect. A large-scale clinical trial (the UK Prospective Diabetes Study [UKPDS] 34) has shown that metformin therapy decreased the risk of cardiovascular death and the incidence of myocardial infarction associated with diabetes mellitus,[1] suggesting that this drug may be useful for patients who have both cardiovascular disease and diabetes mellitus. Eurich and colleagues[2] recently reported the results of a meta-analysis showing that metformin was the only antidiabetic agent to reduce all-cause mortality without causing any harm in patients who had heart failure and diabetes mellitus. These results suggest that a tight link exists between cardiovascular disease and diabetes mellitus and that metformin has a cardioprotective effect. Metformin is known to activate AMP-activated protein kinase (AMPK),[3–5] which is expressed in various tissues, including the myocardium, and plays a central role in the regulation of energy metabolism under stress conditions.[6] AMPK is activated by ischemia/reperfusion,[7–9] as well as in hearts with pressure overload hypertrophy[10] and subsequent heart failure.[11,12] In addition, Russell et al[9] have demonstrated that isolated hearts of AMPK-deleted mice show increased apoptosis and dysfunction after ischemia/reperfusion. Activation of AMPK by adiponectin also has been reported to protect cardiomyocytes against apoptosis and to attenuate myocardial ischemia/reperfusion injury in mice.[8] Furthermore, metformin has been reported to increase the production of nitric oxide (NO),[13–15] which is known to have various beneficial cardiovascular

Received August 23, 2007; accepted February 24, 2009.

From the Department of Cardiovascular Medicine, National Cardiovascular Center (H.S., H.A., H.T., M.W., S.I., A.O., M.A., J.K., K.K., M.K.) and Departments of Structural Analysis (H.S., H.T., M.W., S.I., N.M.) and Cardiovascular Dynamics (M.S., K.K.), Research Institute, National Cardiovascular Center, Suita, Osaka; Departments of Bioregulatory Medicine (H.S., H.T., M.W., S.I., N.M.) and Cardiovascular Medicine (M.F., T.M., S.T., S.S.), Osaka University Graduate School of Medicine, Suita, Osaka, Japan; and Department of Emergency Room Medicine, Kinki University School of Medicine, Osaka-Sayama (H.A.), Osaka, Japan.

The online-only Data Supplement is available with this article at http://circ.ahajournals.org/cgi/content/full/CIRCULATIONAHA.108.798561/DC1.

Correspondence to Masafumi Kitakaze, MD, PhD, Department of Cardiovascular Medicine, National Cardiovascular Center, 5–7–1 Fujishirodai, Suita, Osaka 565–8565, Japan. E-mail kitakaze@zf6.so-net.ne.jp

Circulation **is available at http://circ.ahajournals.org** **DOI: 10.1161/CIRCULATIONAHA.108.798561**

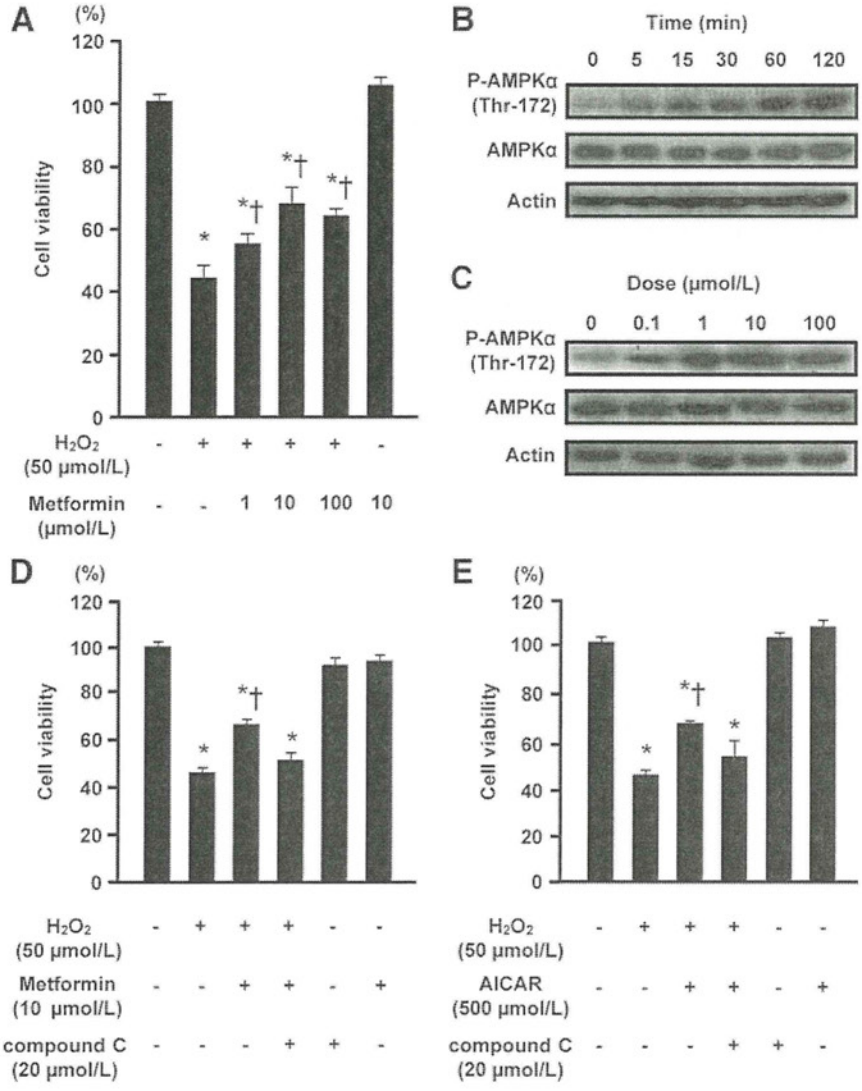

Figure 1. Effect of metformin on oxidative stress–induced cell death via AMPK activation in cultured rat cardiomyocytes. A, Cardiomyocyte viability after treatment with metformin (1, 10, or 100 μmol/L) and exposure to H_2O_2 (50 μmol/L). B, Time (0, 5, 15, 30, 60, 120 minutes) -dependent changes in AMPK phosphorylation in cardiomyocytes after treatment with metformin (10 μmol/L). C, Dose-dependent changes in AMPK phosphorylation in cardiomyocytes after treatment with metformin (0.1, 1, 10, or 100 μmol/L). D, Effect of an AMPK inhibitor (compound C; 20 μmol/L) on cardiomyocyte viability after treatment with metformin (10 μmol/L). E, Effect of an AMPK activator (AICAR; 500 μmol/L) on cardiomyocyte viability after treatment with metformin (10 μmol/L). Values are mean±SEM. P-AMPKα indicates phosphorylation of AMPKα. *$P<0.05$ vs no treatment; †$P<0.05$ vs H_2O_2 (50 μmol/L) treatment.

effects[16] and may alleviate mechanical or neurohormonal stress on the heart.

Clinical Perspective on p 2577

These findings led us to hypothesize that activation of AMPK by metformin may exert a cardioprotective effect under stress conditions. Accordingly, metformin might be a potential new treatment for cardiac failure because it activates AMPK and increases NO production. Therefore, we investigated the influence of metformin on apoptosis, an important feature of heart failure, using cultured neonatal cardiomyocytes exposed to H_2O_2 and the effect of metformin on the progression of pacing-induced heart failure in dogs, along with activation of AMPK.

Methods

Experimental procedures are described in the online-only Data Supplement.

Statistical Analysis

Results are expressed as mean±SEM. Comparison of changes between groups over time was performed by 2-way repeated-measures ANOVA. Other data were compared between groups by 1-way fractional ANOVA. The Tukey-Kramer test was used to correct for multiple comparisons. In all analyses, values of $P<0.05$ were considered to indicate statistical significance.

The authors had full access to and take full responsibility for the integrity of the data. All authors have read and agree to the manuscript as written.

Results

Metformin Attenuates Oxidative Stress–Induced Cell Death and Apoptosis in Cultured Cardiomyocytes via AMPK Activation

Cell viability was decreased in the presence of H_2O_2, as shown by the MTT assay, but this change was blunted by treatment with metformin in a dose-dependent manner (Figure 1A). Treatment with metformin (10 μmol/L) stimulated phosphorylation of AMPK in cultured cardiomyocytes in a time- and dose-dependent manner (Figure 1B and 1C). The effect of metformin on cell viability was blunted by cotreatment with compound C, an AMPK inhibitor (20 μmol/L) (Figure 1D). 5-Amino-4-imidazole-1-β-D-carboxamide ribofuranoside (AICAR; another AMPK activator) had an effect similar to metformin on cardiomyocyte viability after exposure to H_2O_2 (Figure 1E). These results suggested that